AD-A066 041 NAVAL OCEAN SYSTEMS CENTER SAN DIEGO CA F/G 9/3
TWO-DIMENSIONAL PROCESSING FOR ACOUSTIC SIGNAL SPACE IMAGERY.(U)
DEC 78 J A ROESE
UNCLASSIFIED NOSC/TR-337 NL

1 OF 1
AD A066041

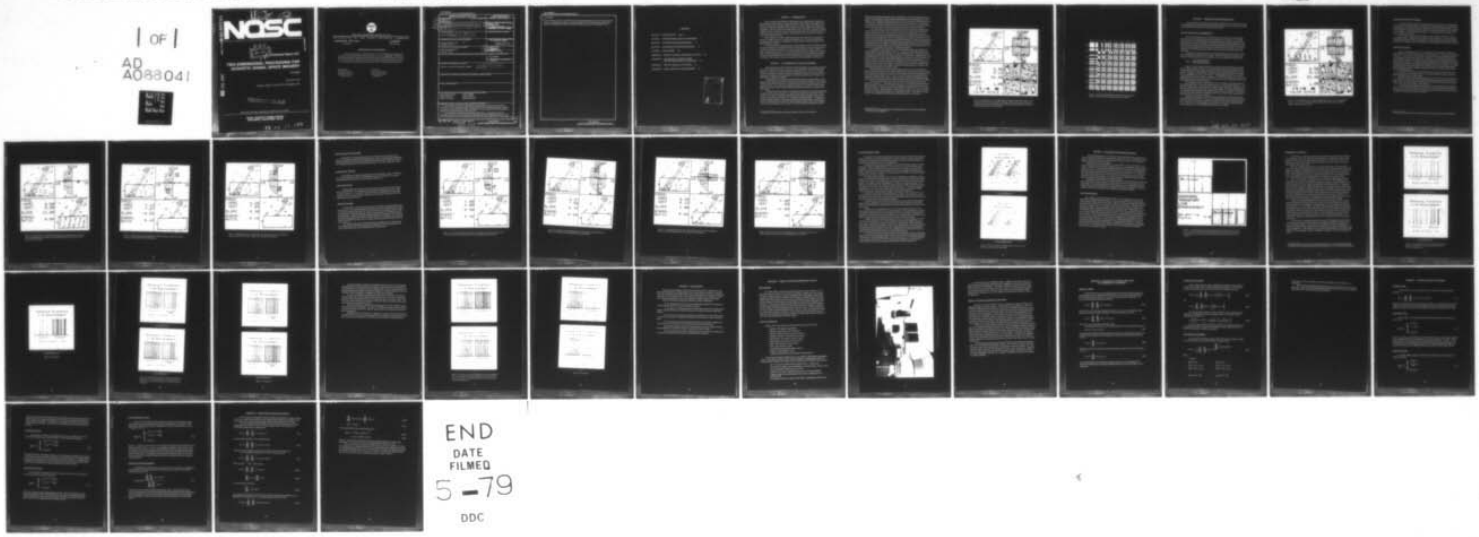

END
DATE FILMED
5-79
DDC

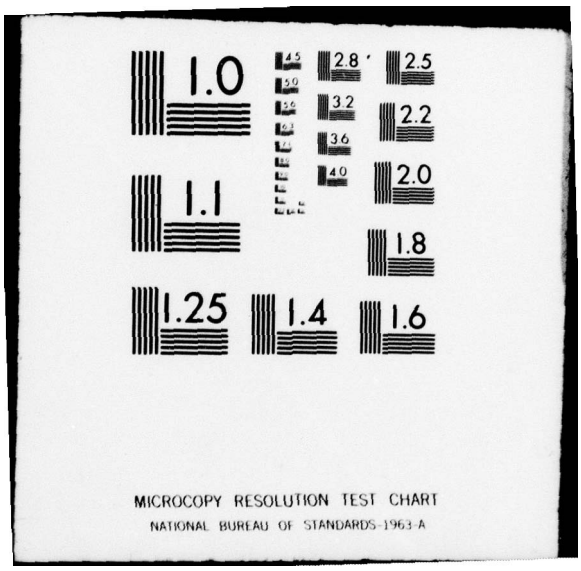
1.0
1.1
1.25
1.4
1.6
1.8
2.0
2.2
2.5
2.8
3.2
3.6
4.0
MICROCOPY RESOLUTION TEST CHART
NATIONAL BUREAU OF STANDARDS-1963-A

LEVEL II

NOSC

Technical Report 337

TWO-DIMENSIONAL PROCESSING FOR ACOUSTIC SIGNAL SPACE IMAGERY

JA Roese

December 1978

Research Report: October 1976 - December 1977

NAVAL OCEAN SYSTEMS CENTER
SAN DIEGO, CALIFORNIA 92152

NAVAL OCEAN SYSTEMS CENTER, SAN DIEGO, CA 92152

AN ACTIVITY OF THE NAVAL MATERIAL COMMAND

RR GAVAZZI, CAPT, USN
Commander

HL BLOOD
Technical Director

ADMINISTRATIVE INFORMATION

This report summarizes work performed for the FY77 IR/IED Two-Dimensional Transform Processing Program, Program Element 61152N, Task ZR01-408. Applicable processing techniques developed under the Naval Electronic Systems Command, ELEX-320 FY77 block program in undersea surveillance have been incorporated into this documentation. This work was performed during the period October 1976 through December 1977.

Reviewed by
D.A. Hanna, Head
Signal Processing and
Display Division

Released by
H.A. Schenck, Head
Undersea Surveillance
Department

UNCLASSIFIED

SECURITY CLASSIFICATION OF THIS PAGE (When Data Entered)

REPORT DOCUMENTATION PAGE

READ INSTRUCTIONS BEFORE COMPLETING FORM

1. REPORT NUMBER: NOSC/TR-337	2. GOVT ACCESSION NO.
3. RECIPIENT'S CATALOG NUMBER	
4. TITLE (and Subtitle): TWO-DIMENSIONAL PROCESSING FOR ACOUSTIC SIGNAL SPACE IMAGERY	5. TYPE OF REPORT & PERIOD COVERED: Technical Research report - Oct 1976 - Dec 77
	6. PERFORMING ORG. REPORT NUMBER
7. AUTHOR(s): JA Roese / J. A. Roese	8. CONTRACT OR GRANT NUMBER(s)
9. PERFORMING ORGANIZATION NAME AND ADDRESS: Naval Ocean Systems Center, San Diego, CA 92152	10. PROGRAM ELEMENT, PROJECT, TASK AREA & WORK UNIT NUMBERS: 1414
11. CONTROLLING OFFICE NAME AND ADDRESS: Naval Ocean Systems Center, San Diego, CA 92152	12. REPORT DATE: December 1978
	13. NUMBER OF PAGES: 40
14. MONITORING AGENCY NAME & ADDRESS (if different from Controlling Office)	15. SECURITY CLASS. (of this report): UNCLASSIFIED
	15a. DECLASSIFICATION/DOWNGRADING SCHEDULE

16. DISTRIBUTION STATEMENT (of this Report)

Approved for public release; distribution unlimited

ZR01408

17. DISTRIBUTION STATEMENT (of the abstract entered in Block 20, if different from Report)

18. SUPPLEMENTARY NOTES

19. KEY WORDS (Continue on reverse side if necessary and identify by block number)

Digital image processing	Acoustic imaging
Image enhancement	Fourier transforms
Image transformations	Hadamard transforms

20. ABSTRACT (Continue on reverse side if necessary and identify by block number)

Many techniques fundamental to digital image processing hold great potential for the analysis and enhancement of acoustic signal space images. Applications of this body of image processing theory and analysis techniques to acoustic signal space imagery are investigated. These techniques provide a fundamentally new approach to information extraction for this class of data.

The basic elements of digital image processing investigated include: two-dimensional Fourier and Hadamard transformations of acoustic signal space images; high-pass, low-pass, band-pass and band-reject transform domain filtering and pattern modification operations; and inverse image transformations. These transform

→ next page

DD FORM 1 JAN 73 1473 EDITION OF 1 NOV 65 IS OBSOLETE S/N 0102-LF-014-6601

UNCLASSIFIED

SECURITY CLASSIFICATION OF THIS PAGE (When Data Entered)

393 159

20. Continued

domain operations are shown to be effective tools for the isolation, suppression and enhancement of features of interest in acoustic signal space imagery. The results obtained show that the techniques of two-dimensional transform processing gives the acoustic image analyst a versatile and powerful set of investigative tools.

CONTENTS

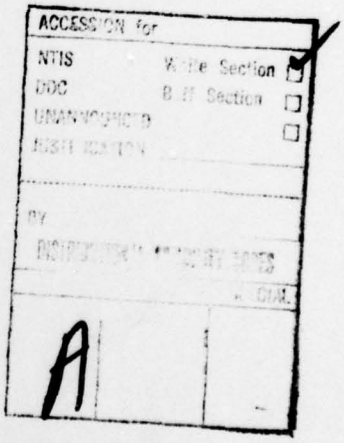

SECTION 1 – INTRODUCTION

Many techniques fundamental to digital image processing hold great potential for the analysis and enhancement of acoustic signal space images. Historically, applications of image processing have addressed problems relating to natural images and include image coding for bandwidth compression, edge detection and feature enhancement, spatial noise suppression, and corrections for image distortions due to motion blur or optical aberrations. Application of this well-defined body of image processing theory and analysis techniques to acoustic signal space imagery represents a fundamentally new approach to information extraction for this class of data.

Many problems in acoustic signal detection and extraction involve the analysis of patterns or spatial features in a two-dimensional signal space. The tools of digital image processing provide a means for establishing a solid theoretical and mathematical basis for dealing with such problems.

The basic elements of digital image processing employed in this investigation include: two-dimensional Fourier and Hadamard image transformations; transform domain filtering and pattern modification operations; and inverse transformations to isolate, suppress, or enhance signal features of interest. The results obtained provide an assessment of the feasibility of applying digital image processing to the analysis of acoustic signal space imagery. The display and processing resources of the NOSC Display and Image Processing Facility and Univac 1108 computer were used in obtaining the results presented in this report.†

SECTION 2 – TWO-DIMENSIONAL IMAGE TRANSFORMS

The underlying concept of transform domain processing is that a discrete representation of the input or source acoustic data array, $f(x,y)$ undergoes a two-dimensional transformation to produce an array of transform coefficients, $F(u,v)$, where u,v are spatial frequency coordinates. Transform domain decomposition is based on the premise that an image can be considered as the superposition of multiple transform basis functions, each with different weighting coefficients.

Computation of a two-dimensional transform produces a decomposition of the source acoustic image in terms of horizontal and vertical spatial frequencies. The transform domain image representation gives a two-dimensional distribution of image energy at each spatial frequency. The location and magnitude of peaks in the transform domain energy distribution provides a direct means of measuring parameters of features contained in the source image.

For transform domain image representations, the transform is normally chosen from the class of linear unitary operators, i.e., operators [T] having the property that $[T][T]^* = [T]^*[T] = [I]$, where * denotes the conjugate transpose of the complex operator. When restricted to real-valued variables, [T] is termed an orthogonal operator. Properties of unitary transforms include: preservation of length under transformation; transformation of sets of orthonormal basis vectors into other orthonormal basis vectors; and transformation of sums of squares into sums of squares. This latter property implies that the total

†A description of the NOSC Display and Image Processing Facility is given in Appendix A.

energy in both domains is preserved under transformation. Unitary transformations commonly used in transform domain image processing include the Karhunen-Loeve, cosine, Fourier, slant, Hadamard, and Haar transforms. With the exception of the Karhunen-Loeve transform, fast computational algorithms are known for each transform. The Karhunen-Loeve transform produces completely uncorrelated components in the transform domain, whereas the other transform types possess varying amounts of residual correlation.

Two main classes of unitary transforms have been investigated for application to acoustic signal space images. These are the discrete Fourier and Hadamard transforms.* The Fourier transform is of interest because it provides a decomposition of the source image in terms of periodic exponential basis functions of increasing spatial frequency. In general, the Fourier transform of an N X N image array is a complex function of size $2N^2$, i.e., the real and imaginary (or magnitude and phase) components at each spatial frequency. However, because of the complex conjugate symmetry properties of the Fourier transform, only half of the real and imaginary (or magnitude and phase) components are required for complete image reconstruction. Thus, the two-dimensional Fourier transform of an N X N image array is completely defined by N^2 transform components.

An example of the application of two-dimensional transform processing of an acoustic signal space image is given in Figure 2-1. In this figure, the source image, f(x,y), is displayed in the upper left quadrant. The two-dimensional Fourier transform domain energy distribution for the source image is shown at the upper right. A magnified view (2:1 expansion) about the origin of the energy distribution is presented at the lower right. This data set illustrates several well-defined transform domain energy concentrations. The existence of these energy concentrations is significant since it indicates the presence of multiple features in the source image. From the locations and relative strength of the transform domain energy concentrations, quantitative measurements can be made of the major feature parameters in the source image.

The second class of unitary transformations considered is the two-dimensional discrete Hadamard transform. This transform differs from the more familiar Fourier transform in that, instead of periodic complex exponential basis functions, the Hadamard transform basis functions assume only ±1 values. A desirable property resulting from the Hadamard transform basis functions is that hardware for performing Hadamard image transformations can be implemented using only simple addition and subtraction operations.

The first eight horizontal, vertical, and off-axis Hadamard basis functions are illustrated in Figure 2-2. This figure shows that the set of Hadamard basis functions is slightly aperiodic in nature but are ordered according to increasing number of axis crossings (sign changes). These properties of the Hadamard transform have led to the introduction of the term "spatial sequency," where sequency refers to the number of basis function axis crossing (sign changes) for a nonperiodic function. In the case of a periodic function, the concepts of spatial sequency and spatial frequency are identical.

*The mathematical relationships defining the two-dimensional forms for the Fourier and Hadamard transforms are given in Appendix B.

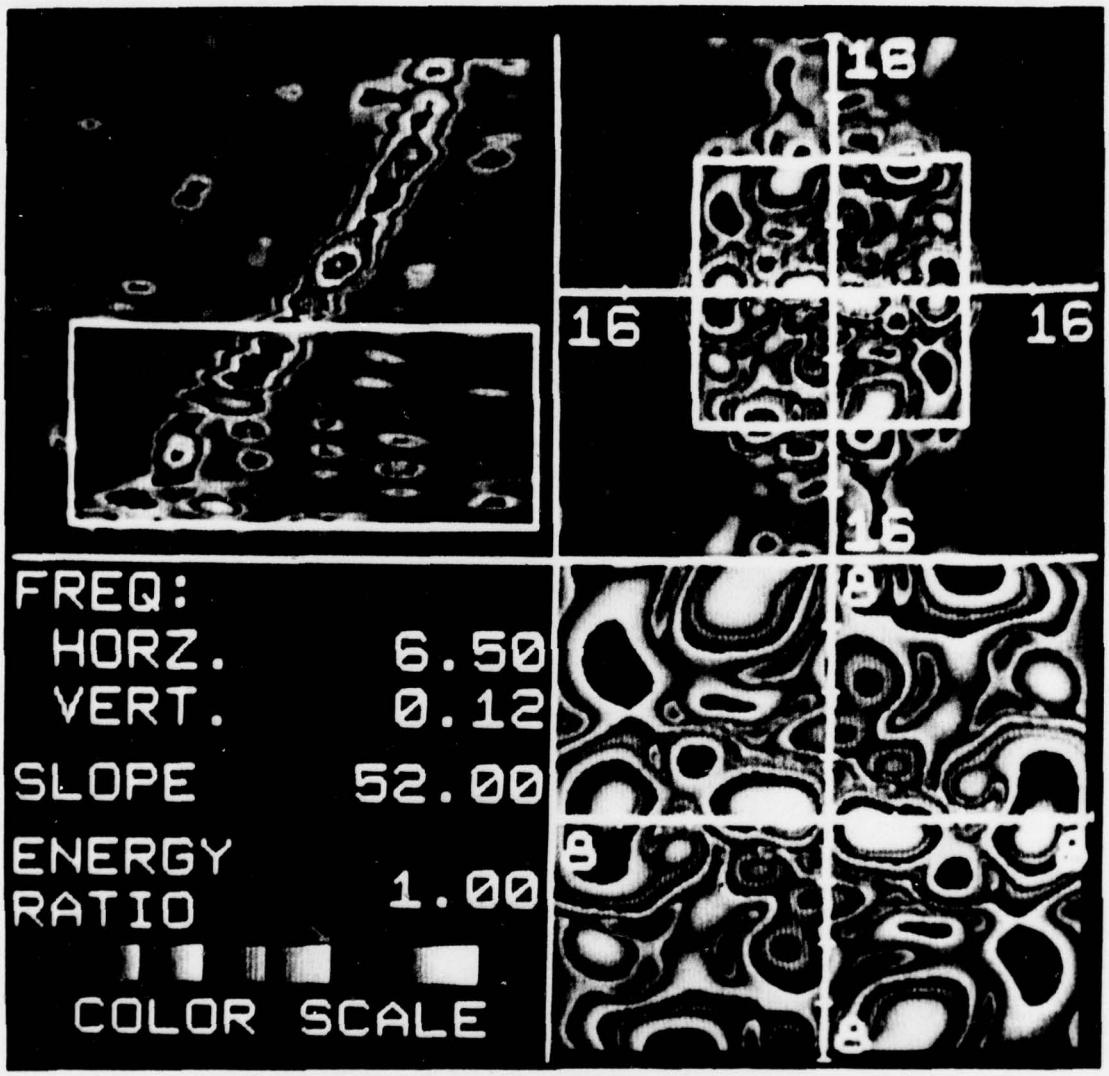

Figure 2-1. Representations of the original image, its two-dimensional Fourier transform with an expanded view of the central portion of the image transform, and typical feature parameter measurements. The observed transform domain energy concentrations indicate the presence of multiple spatial features in the original image.

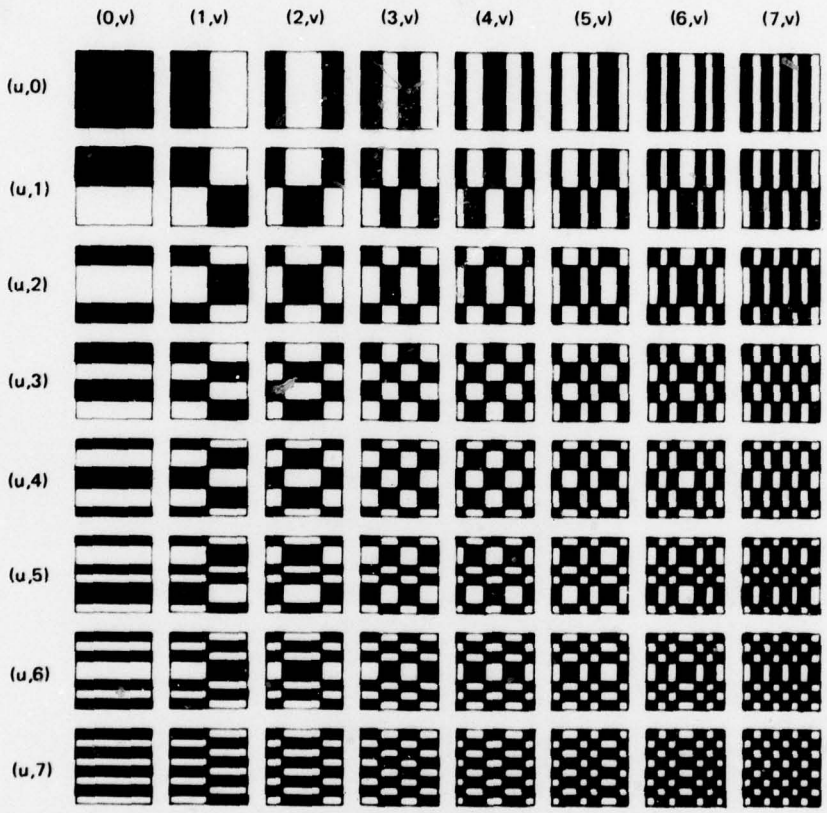

Figure 2-2. Two-dimensional Hadamard transform basis functions for first eight horizontal, vertical and off-axis spatial sequency components.

SECTION 3 – FOURIER TRANSFORM PROCESSING

Fourier transform spatial frequency domain representations are well suited for image processing applications because of the direct analogues which can be drawn with the method of conventional one-dimensional Fourier time series analysis.

SPATIAL FREQUENCY DECOMPOSITION

Much useful information can be obtained by direct measurement of feature parameters made in the transform domain energy distribution of an image. For example, numerical values for horizontal and vertical spatial frequencies can be determined from the locations of energy concentrations in the transform domain energy distribution. These measured values represent the number of times the spatial feature intersects the horizontal and vertical axis boundaries of the transformed portion of the source image. Also, horizontal and vertical spatial periods are obtained as the reciprocals of the measured spatial frequecies.

Measurement of horizontal and vertical spatial periods also permits a direct computation of feature slope within the source image. The slope parameter is a measure of the feature's orientation relative to the coordinates of the source image and is computed as

$$\text{Slope} = \frac{\text{Vertical Spatial Period}}{\text{Horizontal Spatial Period}}$$

Figure 3-1 shows the basic format for two-dimensional transform domain analysis. As in the earlier example of Figure 2-1, the source image is shown at the upper left. The outlined region of the source image defines the portion of the image selected for transformation. For purposes of illustration, a prominent spatial feature within the source image has been highlighted by the use of an overlay. The highlighted feature is one of many features which, when taken together, comprise the total structure of the source image. The highlighted feature has a repetitive structure that intersects the horizontal axis six times and is essentially parallel with the vertical axis.

The magnitude of the two-dimensional Fourier transform energy distribution for the transformed portion of the source image is shown at the upper right of Figure 3-1. Logarithmic scaling is used to compensate for the large dynamic range of the transform magnitude values. Phase information is not shown in this example. The lower right quadrant is a 2:1 expansion about the origin of the transform domain energy distribution. The observed symmetry about the origin in the transform domain is due to the complex conjugate symmetry properties of the Fourier transform.

A complex conjugate pair of X's has been superimposed in the transform domain energy distribution of Figure 3-1. These X's correspond to the overlay on the source image and are located at (±6,0) along, respectively, the horizontal and vertical spatial frequency axes. The presence of a large transform domain energy concentration at these locations confirms the presence of the highlighted feature in the source image.

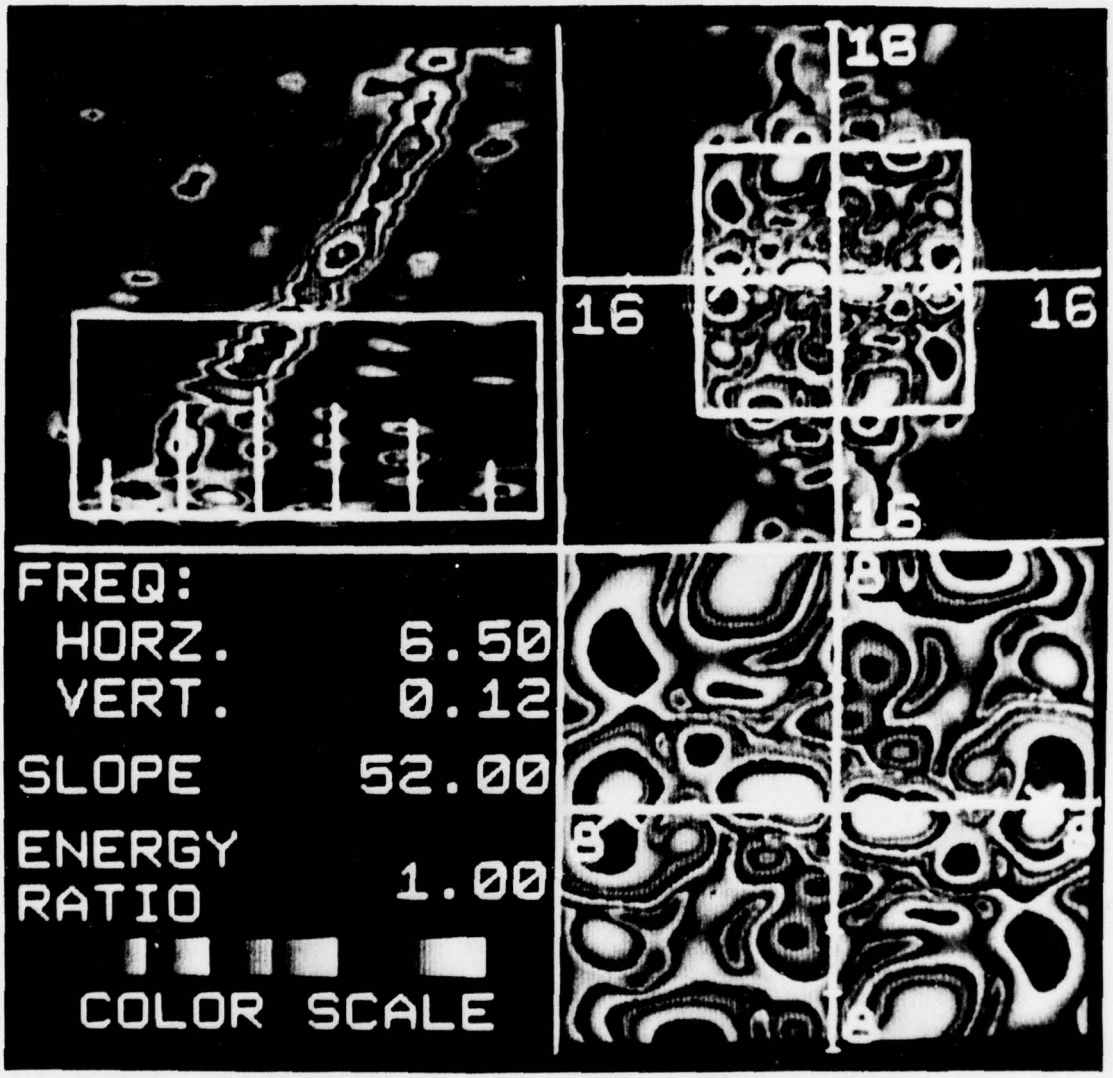

Figure 3-1. Two-dimensional Fourier transform domain analysis format. The overlay highlights a major feature in the source image, and the X's indicate the location of the corresponding transform domain energy concentration.

SPATIAL FREQUENCY FILTERING

Frequency domain image representations provide a useful format for manipulating the properties of the source image. For example, the familiar concepts of one-dimensional frequency domain filtering can be directly applied to the two-dimensional spatial frequency decompositions of acoustic signal space images. Two-dimensional spatial frequency filters can be applied in the transform domain prior to reconstructing the source image by an inverse transform operation.*

Specification of spatial frequency filters is done in a highly interactive manner by the display operator. Filtering options available include selection of: low-pass, high-pass, band-pass and band-reject filters; rectangular or contour-following filter geometry; single or multiple filter implementations; and specification of filter position in the transform domain.

BAND-PASS FILTERS

Figure 3-2 illustrates the use of a two-dimensional band-pass filter to isolate the horizontally repetitive feature shown by the overlay in Figure 3-1. To perform this filtering operation, it was necessary to interactively specify filter bounds and position the filter on the energy concentration of the feature. In this case, a very narrow two-dimensional band-pass filter was used. The results of the filtering procedure are illustrated in the upper right quadrant of Figure 3-2. In this quadrant, the spatial frequency magnitude components outside of the rectangular band-pass filter bounds have been set to zero. Due to the complex conjugate symmetry about the origin in the transform domain, the upper right quadrant shows the spatial frequency magnitude components both prior to and after the transform domain filtering operation.

The filtered reconstruction of the image is shown at the lower right. Within the transformed portion of the image, the effect of band-pass filtering has been to isolate the horizontal feature from the source image.

Another example of band-pass filtering is shown in Figure 3-3. This case illustrates the isolation of one of the major off-axis high spatial frequency components of the source image. From the filtered image reconstruction, the high repetition rate and orientation of this feature can be easily observed and measured.

A third major high-repetition-rate feature of the source image has been isolated in Figure 3-4. The energy concentration for this feature is located in a different quadrant of the transform domain. The feature's structure and orientation relative to the source image are apparent in the filtered image reconstruction.

*The mathematical development of the various types of spatial frequency filters is given in Appendix C.

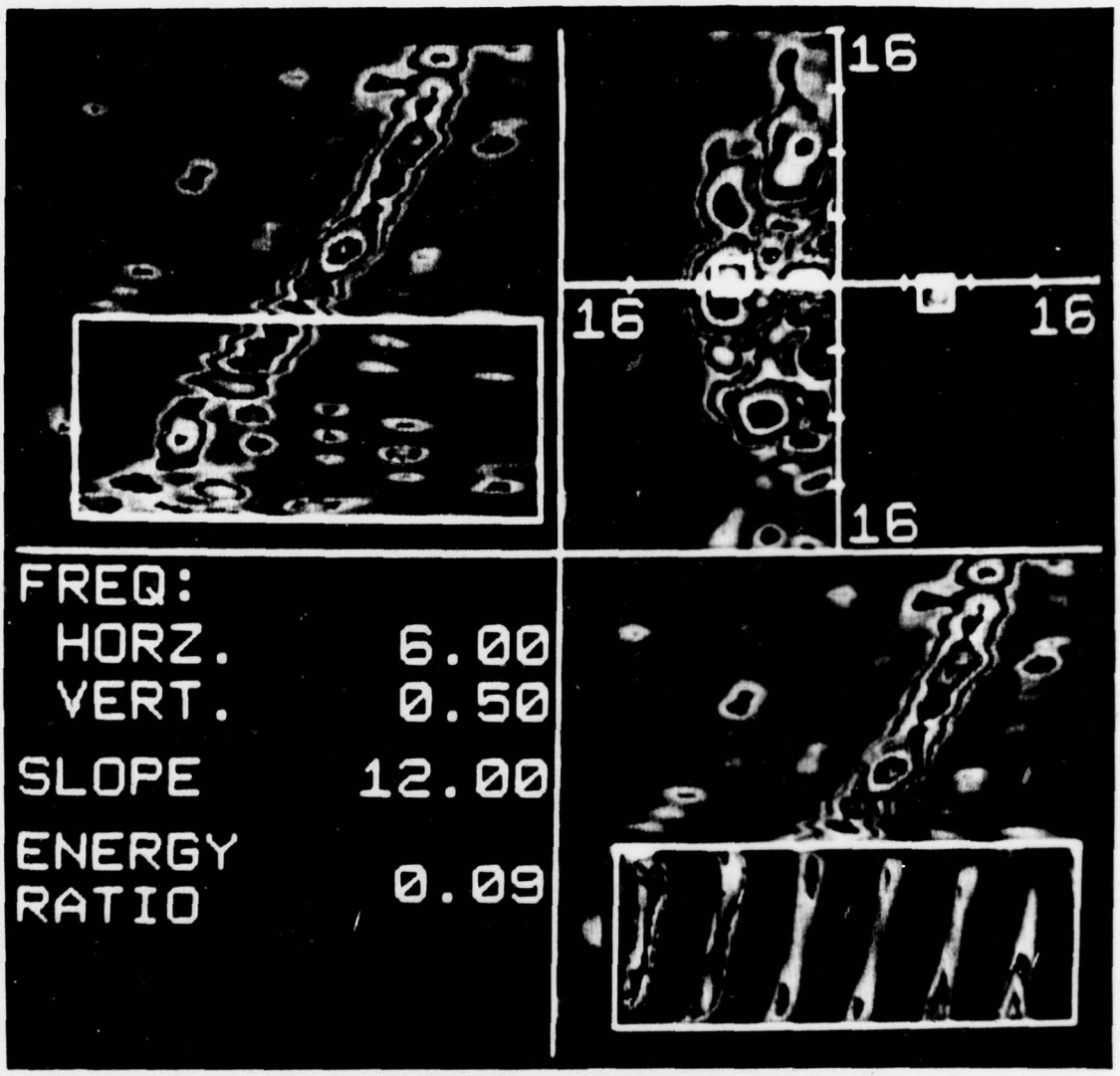

Figure 3-2. Spatial frequency two-dimensional band-pass filter showing the energy concentration and corresponding image reconstruction for the horizontally repetitive feature in the outlined portion of the source image.

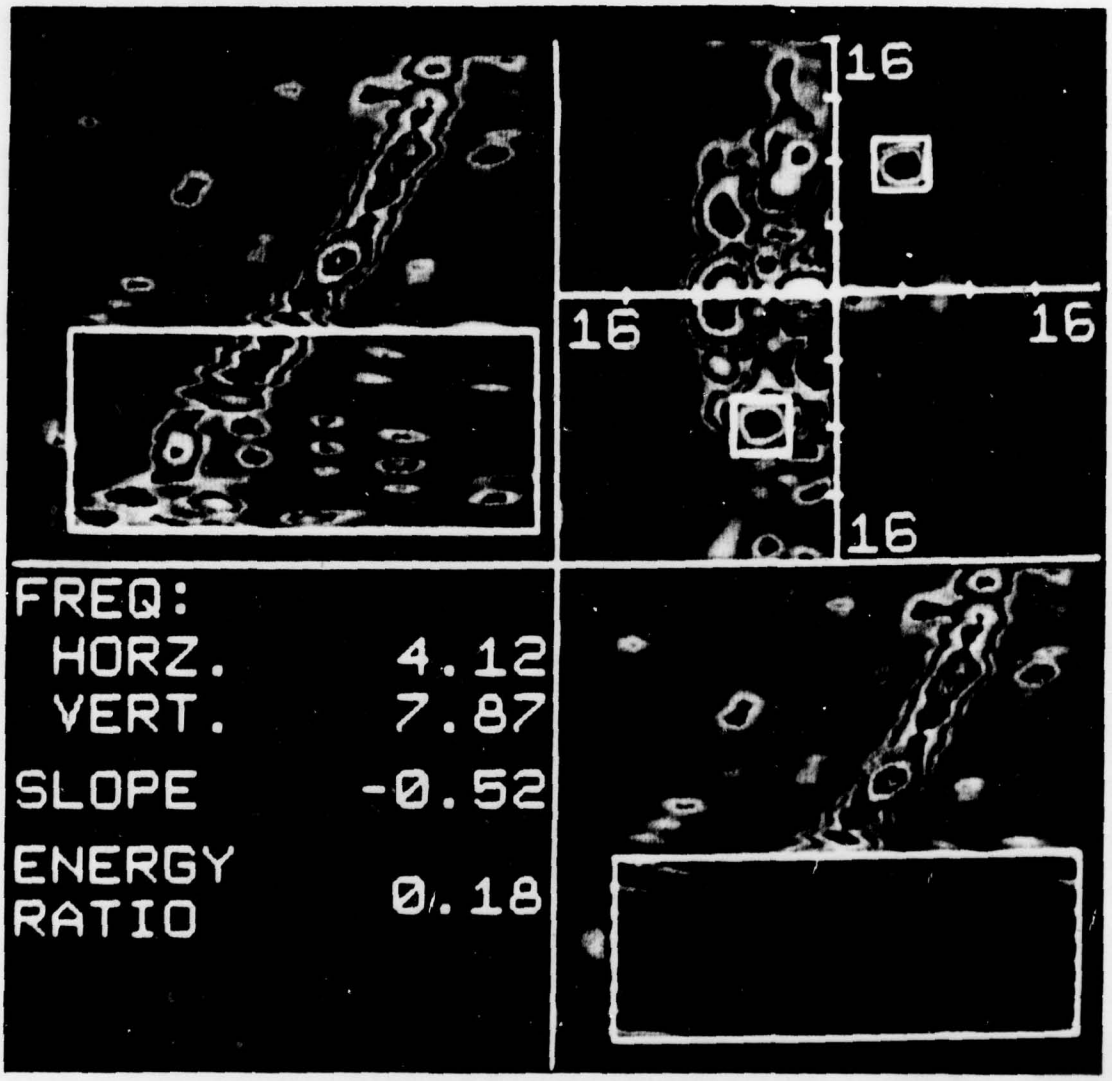

Figure 3-3. High-spatial-frequency band-pass filter. The filtered image reconstruction illustrates the structure and orientation of the isolated feature.

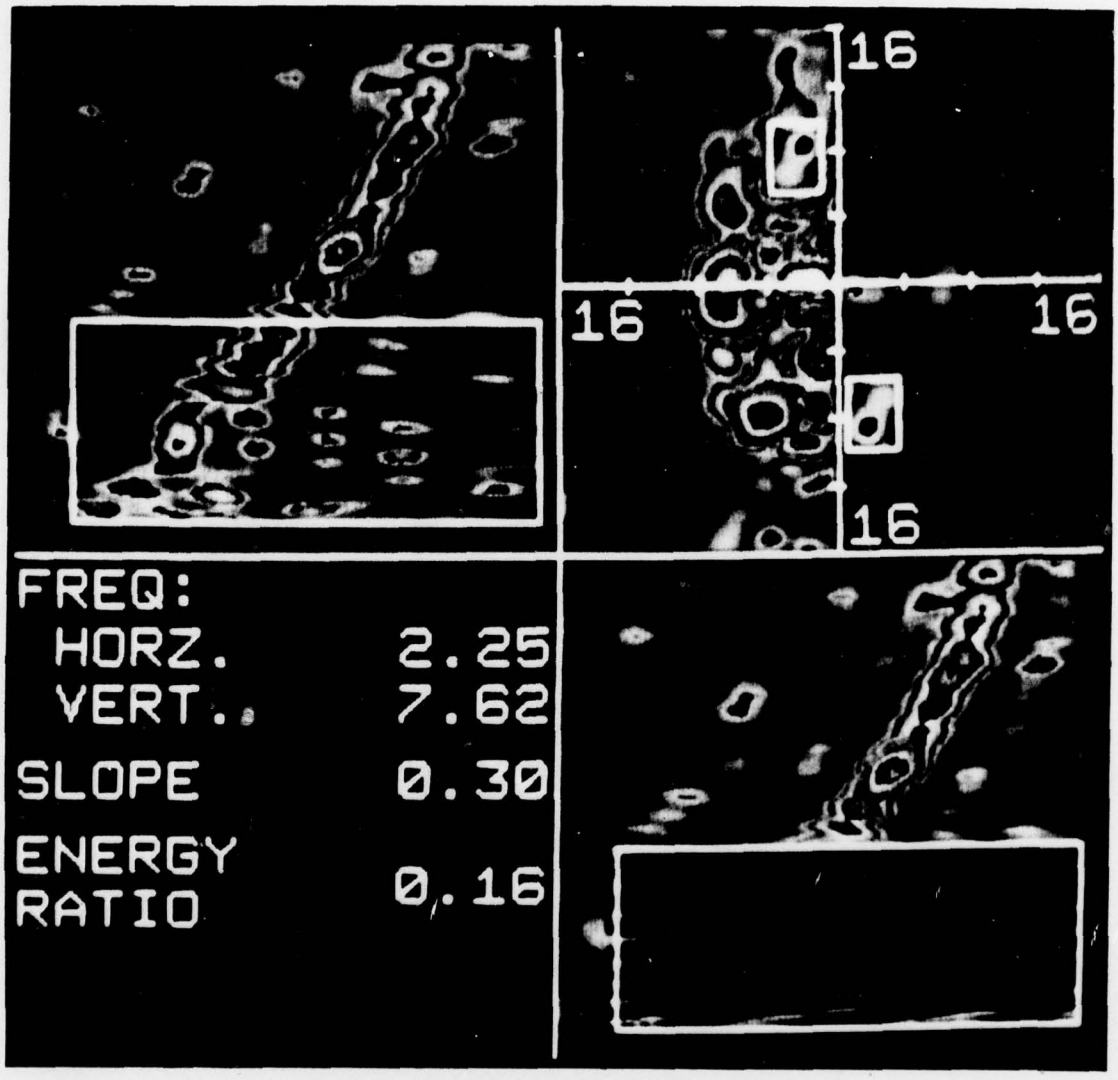

Figure 3-4. High spatial frequency band-pass filter. The filtered image reconstruction illustrates a similar feature structure to that of Figure 3-3 but with different orientation.

MULTIPLE BAND-PASS FILTERS

Combinations of band-pass spatial frequency filters can be effectively used to analyze interactions between individual image features. Figure 3-5 illustrates the application of dual band-pass filters to the two major high-repetition-rate features of Figures 3-3 and 3-4. This example shows that much of the repetitive structure in the source image can be attri-

BAND-REJECT FILTERS

The complement of band-pass filtering is band-reject filtering. Figure 3-6 illustrates the use of dual band-reject filters. This illustration shows the elimination of two major high-repetition-rate features in the source image reconstruction.

LOW-PASS FILTERS

High-repetition-rate features in the source image can be removed with the application of a low-pass filter. An example of low-pass filtering as applied to the source image is given in Figure 3-7. The image reconstruction after low-pass filtering is noticeably smoothed since all spatial frequency components exceeding the horizontal and vertical filter bounds have been removed.

CONTOUR FILTERS

The technique of contour filtering represents a refinement of the basic filter specification process. In contour filtering, the previously employed rectangular filters are replaced by filter geometries that follow the actual contours of the transform domain energy concentrations. Contour filters permit a more precise delineation of complex energy concentrations than is normally obtainable with rectangular filter techniques. Use of contour filtering requires operator interaction to initially specify the local region of the transform domain to be filtered and then to select a specific energy contour which defines the actual filter geometry.

An example of the contour filtering technique as applied to source image energy concentrations in the transform domain is given in Figure 3-8. In this example, a band-reject contour filter with a non-rectangular geometry is illustrated.

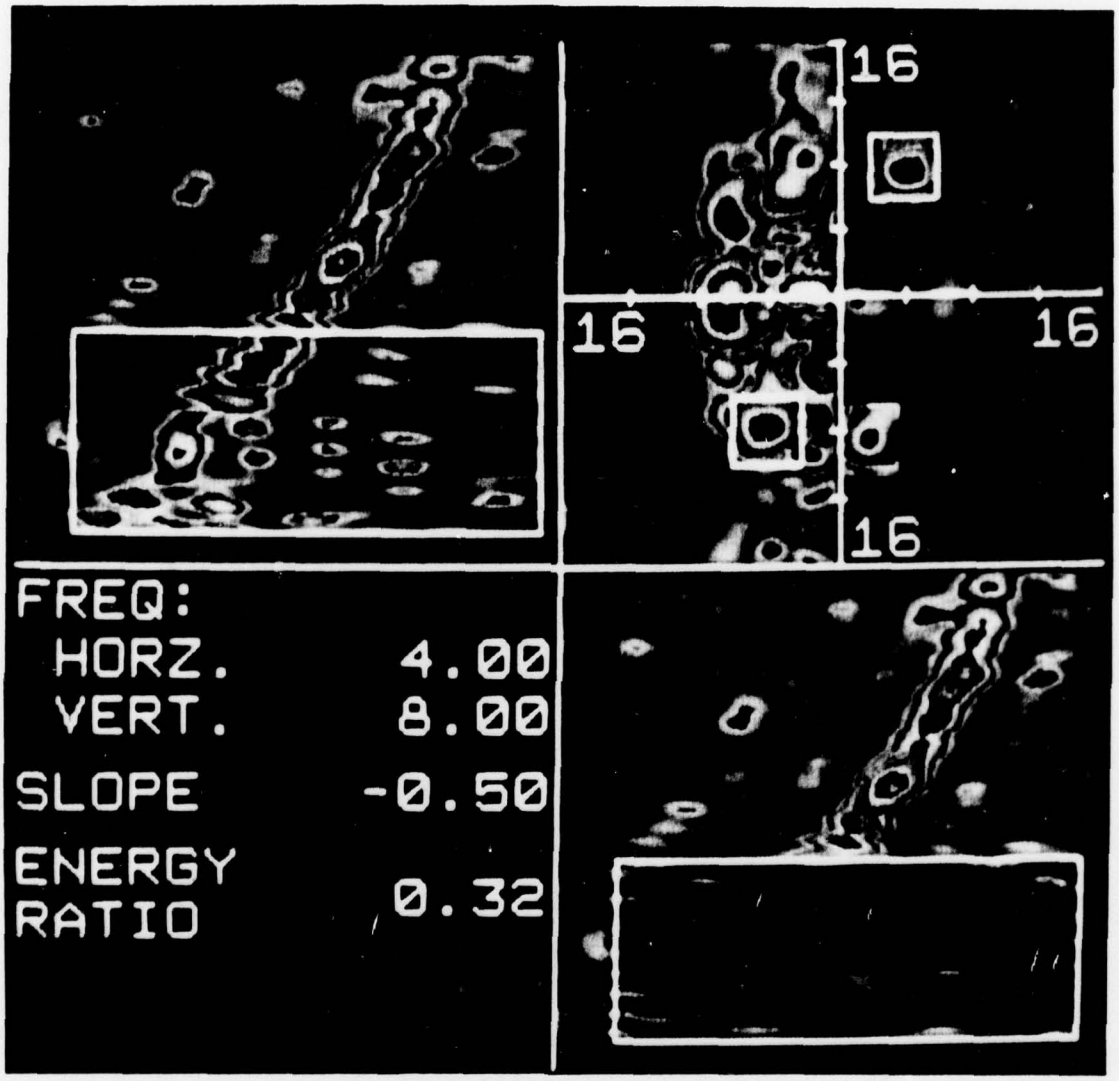

Figure 3-5. Dual band-pass spatial frequency filters. The image reconstruction shows the effects of reinforcement and cancellation between the two major high-repetition-rate features.

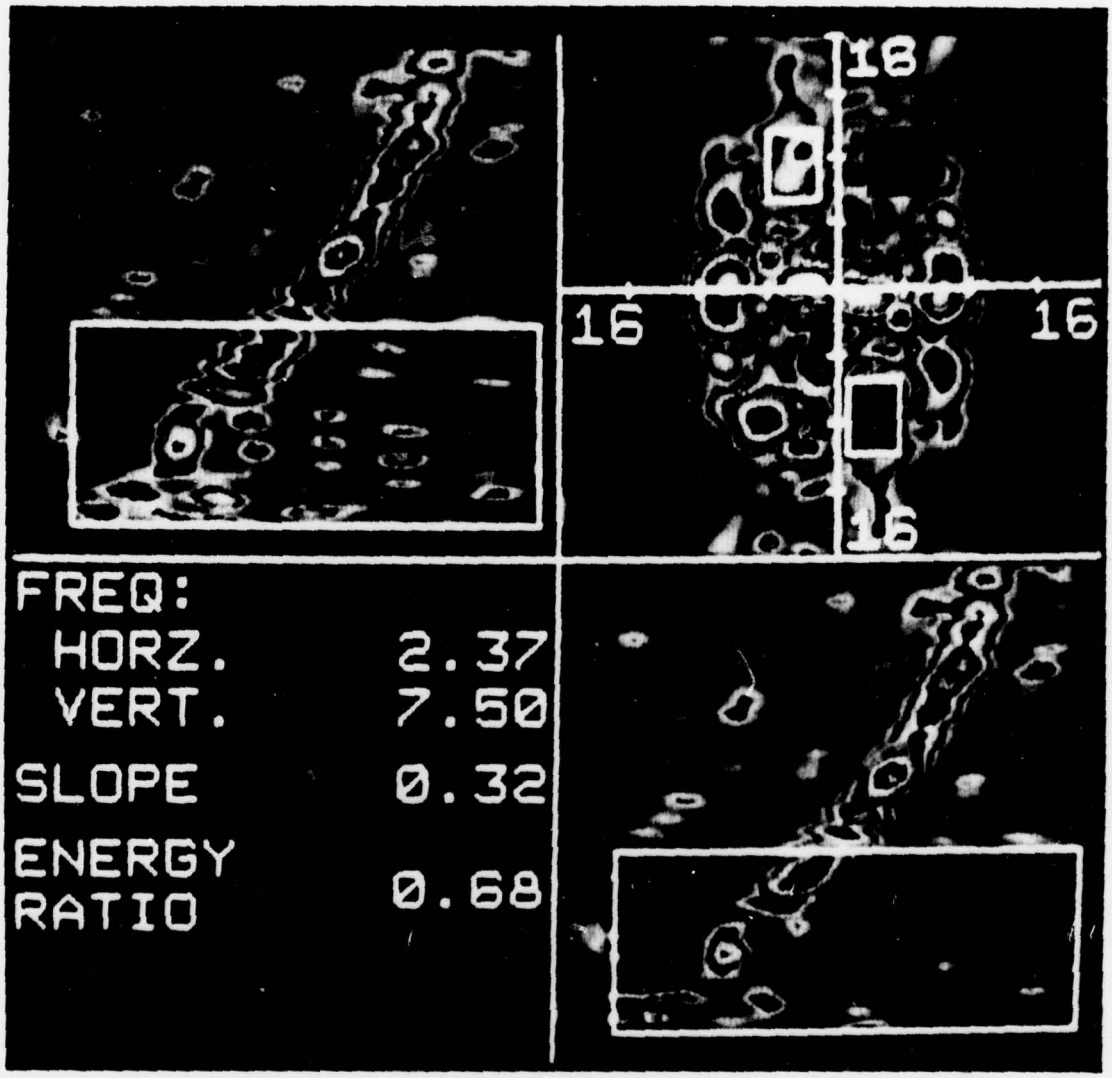

Figure 3-6. Dual band-reject spatial frequency filters. The image reconstruction shows the effects of the removal of the two high-repitition-rate image features.

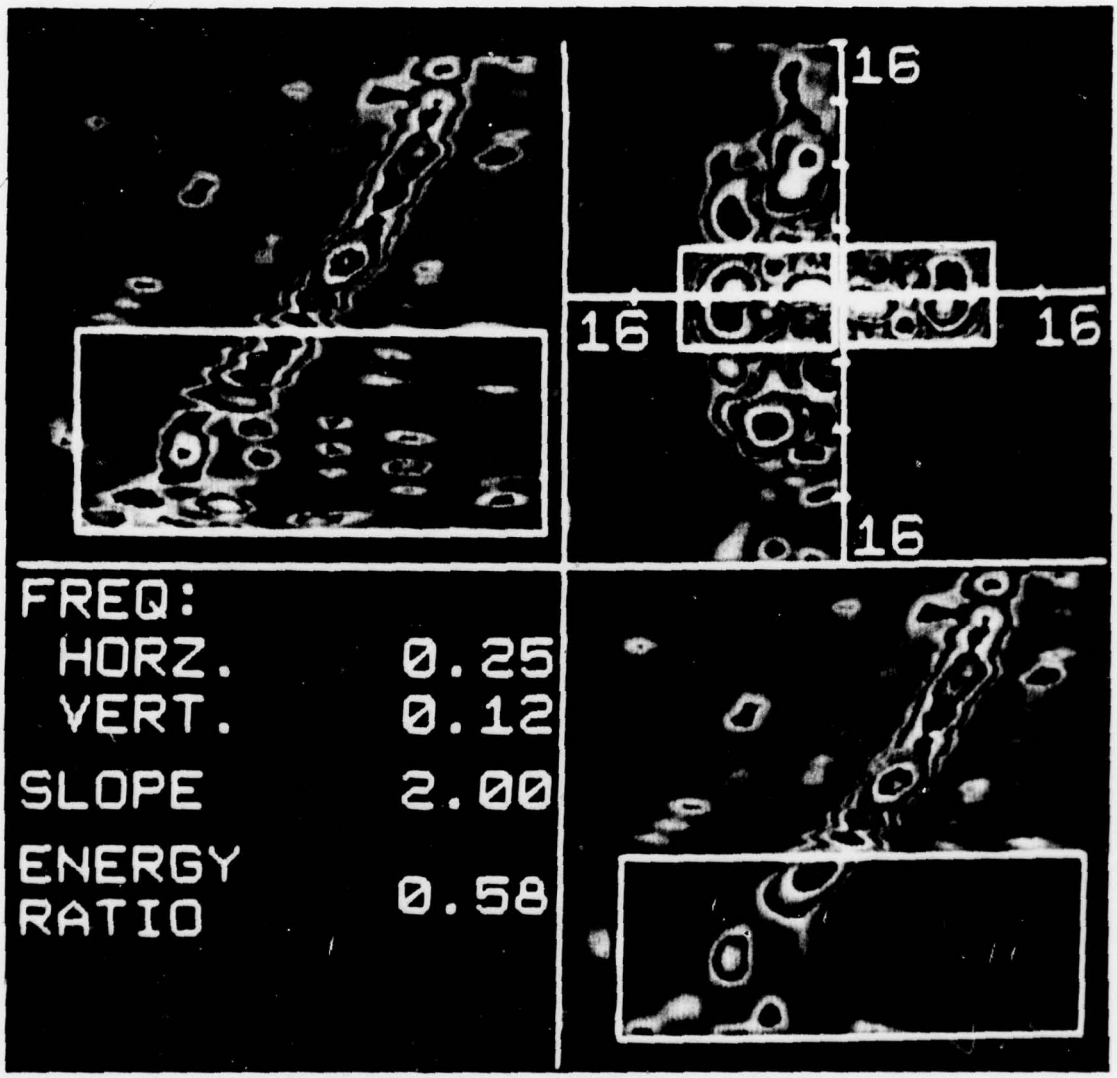

Figure 3-7. Low-pass spatial frequency filter. The reconstruction of the source image appears smooth since the high spatial frequency components have been filtered out.

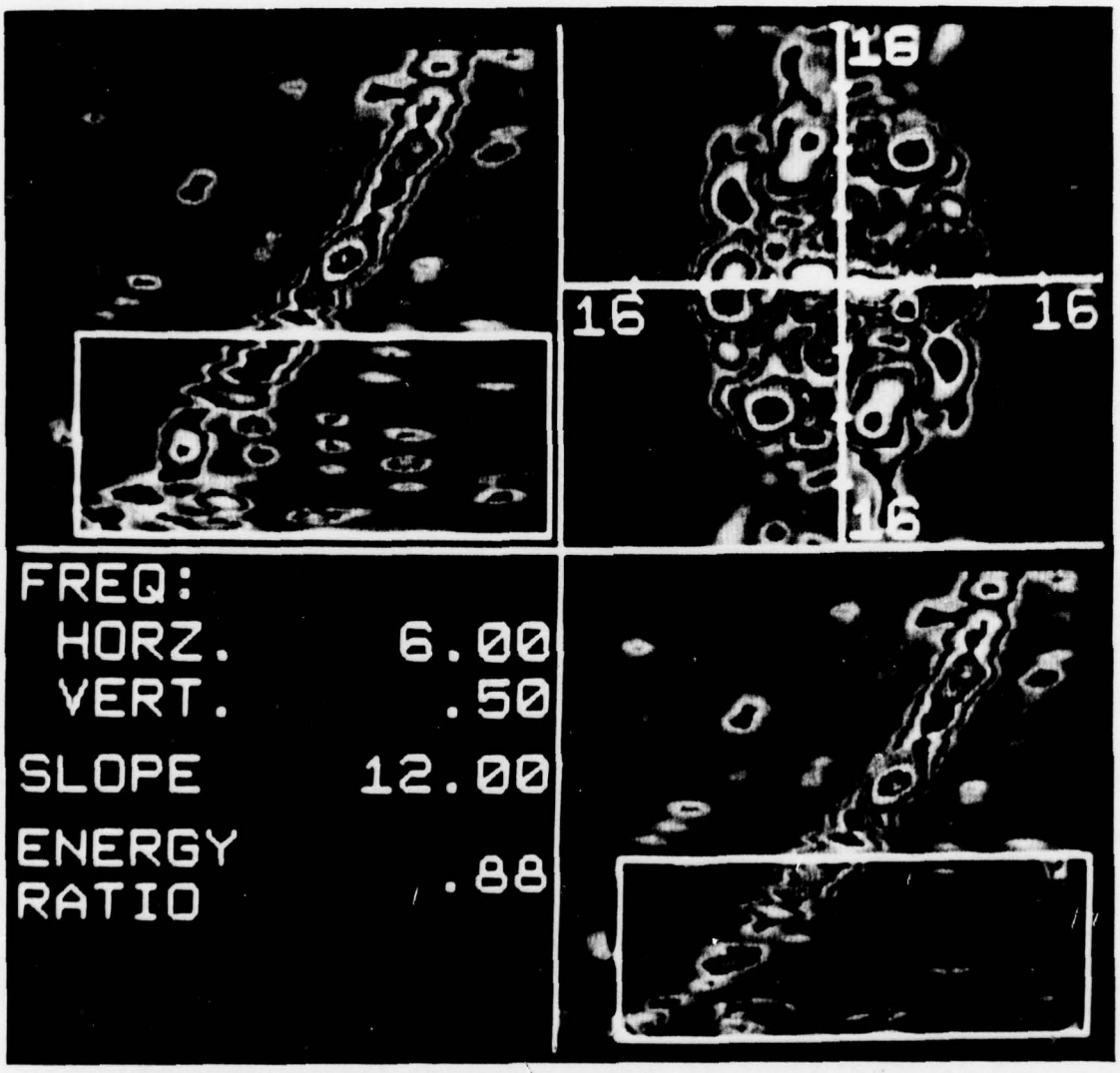

Figure 3-8. Band-reject contour filter. The filter geometry is determined by contours of the transform energy concentration for the high-repetition-rate vertical feature.

PATTERN MODIFICATION

The concept of pattern modification is a direct extension of two-dimensional spatial frequency filtering. In a pattern modification, transform domain energy concentrations corresponding to individual or multiple image features are selectively altered (increased or decreased in strength) prior to inverse transformation.

This approach offers many advantages over conventional spatial frequency filtering techniques, which completely eliminate or zero out the value of certain spatial frequency components. Pattern modification is important because it permits the acoustic image analyst to introduce subtle or major changes in the preceived strength of spatial features or patterns within an image. In many cases, these changes can be made without destroying the basic structure of the source image.

To perform pattern modification, the basic methodologies of high-pass, low-pass, band-pass, and band-reject filtering are used. However, different operator-selectable weighting factors are applied to the spatial frequency components within and outside of the filter bounds. For example, setting a weighting factor of unity for components outside of the filter bounds and less than unity within the bounds results in a relative suppression (but not elimination) of a feature in the resulting image reconstruction. Conversely, setting the weighting factor to a value greater than unity within the filter bounds causes relative enhancement of the perceived feature strength in the image reconstruction.

It should be noted that scaling adjustments are made in the computation of the forward and inverse transforms to insure that the total energy of the input image equals the energy of the output image even though the energy distribution may have been distorted due to the effects of pattern modification operations.

To illustrate the concept of pattern modification, test cases demonstrating spatial feature pattern suppression and enhancement were performed using the source image. Figures 3-9a and b illustrate modifications of the high-vertical-repetition-rate feature in the source image.

In Figure 3-9a, a weighting factor of 0.25 was used within the bounds of a two-dimensional band-pass filter to achieve feature suppression. The spatial frequency components outside of the filter bounds were unchanged. The image reconstruction illustrates a significant de-emphasis in the perceived strength of the vertical-repetition-rate feature in the image reconstruction while preserving the basic structure of the source image.

Another example of pattern modification is that of feature enhancement. This operation is of importance when a feature of interest is present in an image but at a low level. Pattern enhancement provides a technique for increasing the relative strength or detectability of the feature within the context of the original image. An example of pattern enhancement is shown in Figure 3-9b, where a weighting factor of 2.0 is used within the two-dimensional band-pass filter bounds. The resulting image reconstruction presents an enhanced representation of the high-vertical-repetition-rate feature.

The pattern modification process is closely related to spatial frequency filtering and is subject to the same processing considerations that are inherent in two-dimensional inverse transformations for filtering applications. In fact, with the use of a zero-valued weighting factor outside or inside of the filter bounds, pattern modification reduces directly to conventional spatial frequency band-pass and band-reject filtering, respectively.

A.
PATTERN SUPPRESSION

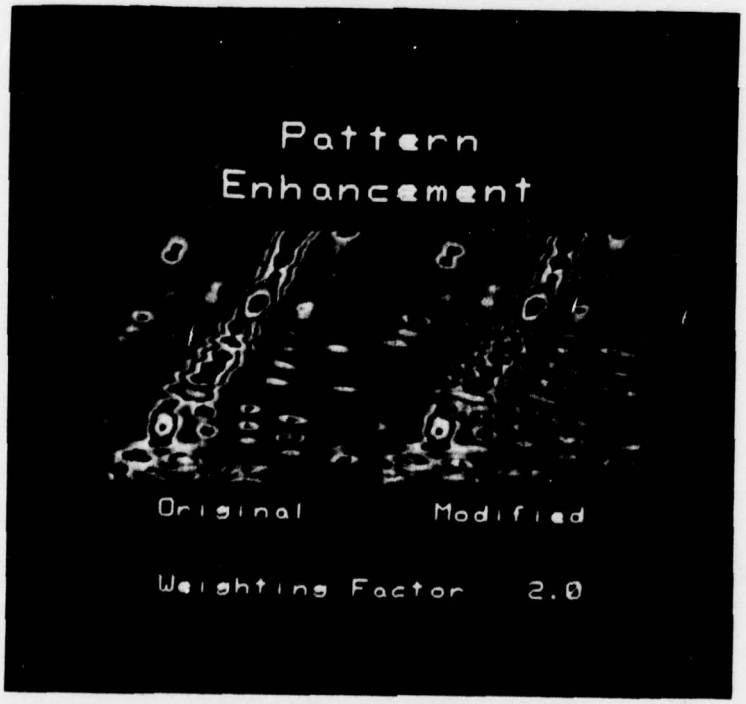

B.
PATTERN ENHANCEMENT

Figure 3-9. Pattern modification technique applied to the high-vertical-repetition-rate feature in the source image.

SECTION 4 – HADAMARD TRANSFORM PROCESSING

The spatial characteristics of the features of interest within an image determine the choice of transform operator to be used for processing. In the case of spectral time history acoustic imagery, the significant image features are known *a priori* to be individual or harmonically related sets of vertical lines.

Operations involving manipulation of vertical lines are not well matched to the complex exponential basis function decompositions of two-dimensional Fourier transformations. However, two-dimensional Hadamard transforms have been successfully applied to vertical line features in spectral time history imagery. By inspection of the Hadamard transform two-dimensional basis functions given previously in Figure 2-2, it can be seen that combinations of the first few rows of these basis functions can provide excellent vertical line feature representations. It is this property of the Hadamard transform which has been exploited for the enhancement of line structures.

It should be noted that the set of Hadamard transform basis functions used will only permit enhancement of lines which are exactly vertical over all or some portion of the source image. Lines which exhibit horizontal variations due to time-dependent frequency changes or have a slope resulting from a constant rate of frequency change will, in general, benefit very little if at all from this class of Hadamard transform techniques.

LINE ENHANCEMENT

The technique of enhancing vertical lines is a direct application of the pattern modification concepts discussed previously. In this case, the patterns of interest are individual and harmonically related vertical lines. Figure 4-1 illustrates the Hadamard transform line enhancement procedure for a spectral time history source image. At the upper left of this figure, a region of the source image has been defined for transform analysis. The Hadamard transform energy distribution is given at the upper right. Careful inspection of the transform energy distribution indicates concentrations of energy along the top few rows of energy components that correspond to the d.c. and low-sequency vertical Hadamard basis functions. These concentrations are caused by the vertical line structures present in the source image. Enhancement of the lines is accomplished by increasing the energy concentration values for the d.c. and low-sequency vertical basis functions prior to reconstructing the image by inverse transformation. In the example of Figure 4-1, a moderate increase in these basis function values results in a significant line enhancement in the image reconstruction. A comparison of an enhanced portion of the image with the original is shown at the lower right of this figure.

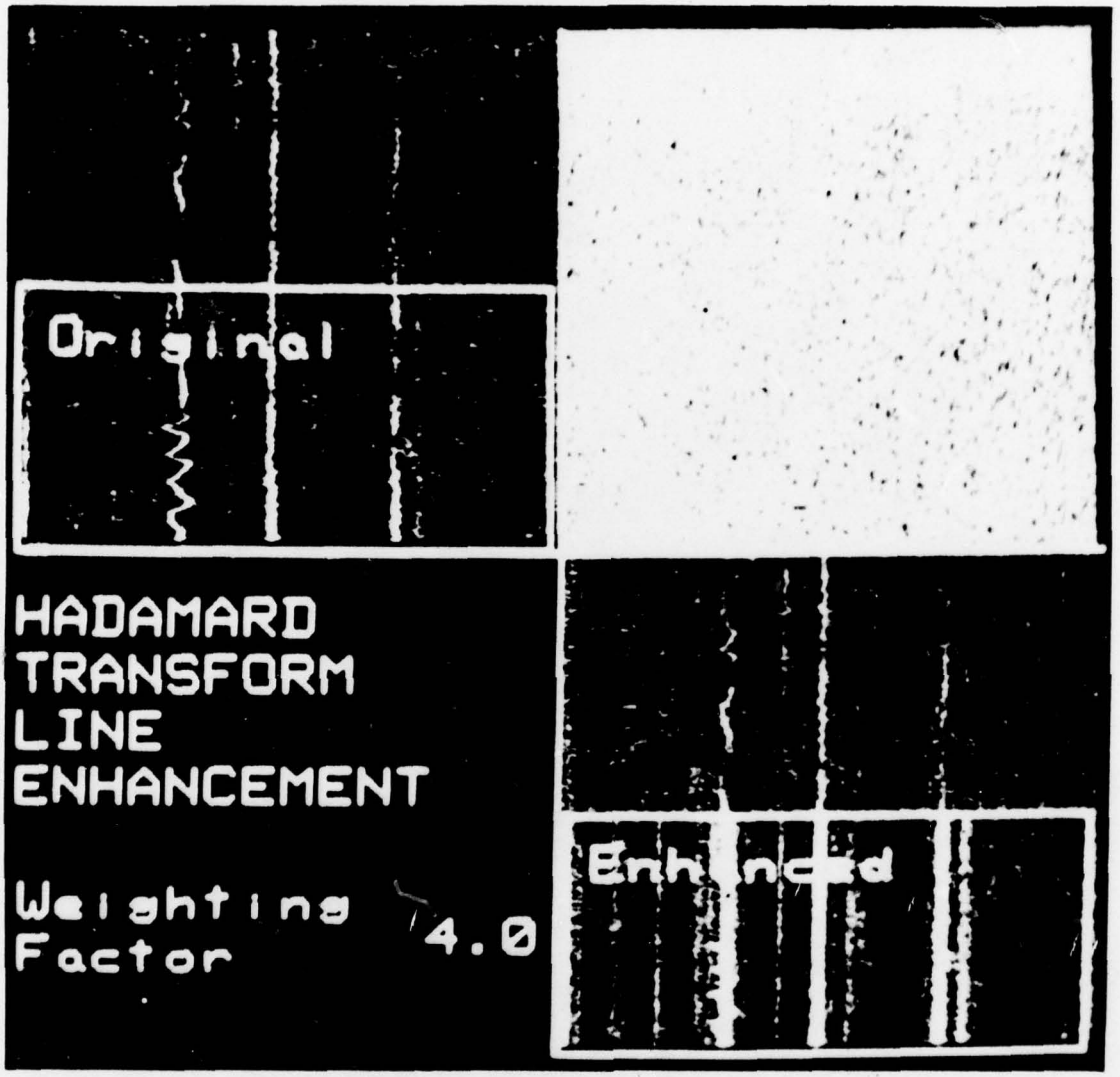

Figure 4-1. Example of Hadamard transform enhancement of vertical lines in the outlined portion of the source image. Line enhancement was achieved by increasing those Hadamard transform energy component values that correspond to line-like structures with a vertical orientation.

EXPERIMENTAL RESULTS

Three different evaluations of the Hadamard transform line enhancement technique were performed. The source image data base used in these evaluations contains several different vertical lines at varying levels of perceptibility. The data base consists of the original source image and four noise-degraded versions of the source image at successively lower signal-to-noise ratios (SNR).

The first evaluation performed was to determine useful d.c. and low-sequency vertical basis function weighting factors for line enhancement. Weighting factors which only slightly exceed unity will essentially preserve the source image and are of little use since they result in only slight line enhancements. Very large weighting factors are also undesirable due to extreme distortion effects in the image reconstruction and the potential for generating line-like artifacts from vertically aligned noise components in the source image.

Figures 4-2a through c illustrate the effects of different weighting factors for the source image. In Figure 4-2a, a weighting factor of 2.0 was used. This weighting factor introduced only a moderate distortion of the Hadamard transform energy distribution and basically preserves the source image with minimal line enhancement effects. A weighting factor of 4.0 was used in the example of Figure 4-2b. The resulting image reconstruction in this case shows a significant increase in the level of line detectability. In particular, certain weak line structures that are essentially undetectable in the source image can be observed in the enhanced image reconstruction. By close examination, the newly observed line structures can be related back to extremely weak lines in the source image. In Figure 4-2c, a high scale factor of 8.0 was used. The distortion in the image reconstruction for this case is severe and has effectively obliterated the detailed structure of the source image.

The second evaluation illustrates that only a small percentage of the d.c. and low-sequency Hadamard transform basis function coefficients actually require adjustment for line enhancement. In this evaluation, a weighting factor of 4.0 was applied to increasing percentages (10, 24, 33 and 100%) of the largest coefficient values along each of the 256 d.c. vertical basis functions. The results of this evaluation are shown in Figures 4-3a through d. These figures indicate that only minor improvements in line enhancement are achieved by weighting more than the largest 25% of the d.c. vertical coefficients. thus, the computational requirements of the Hadamard transform line enhancement technique can be minimized by applying the desired scale factor to only a selected portion of the transform coefficients.

A special case of computational interest occurs with the Hadamard transform line enhancement technique when the scaling factor is applied to all energy components of all d.c. vertical basis functions. In this situation, an operation equivalent to weighting the Hadamard transform energy components can be performed in a column-wise manner on the source image directly. This procedure does not require computation of the two-dimensional transform and, accordingly, results in a significant reduction in the total computational load.*

*The author wishes to acknowledge Dr. Charles Persons, NOSC Code 7132, for making this observation. A mathematical development of the image domain line enhancement procedure is presented in Appendix D.

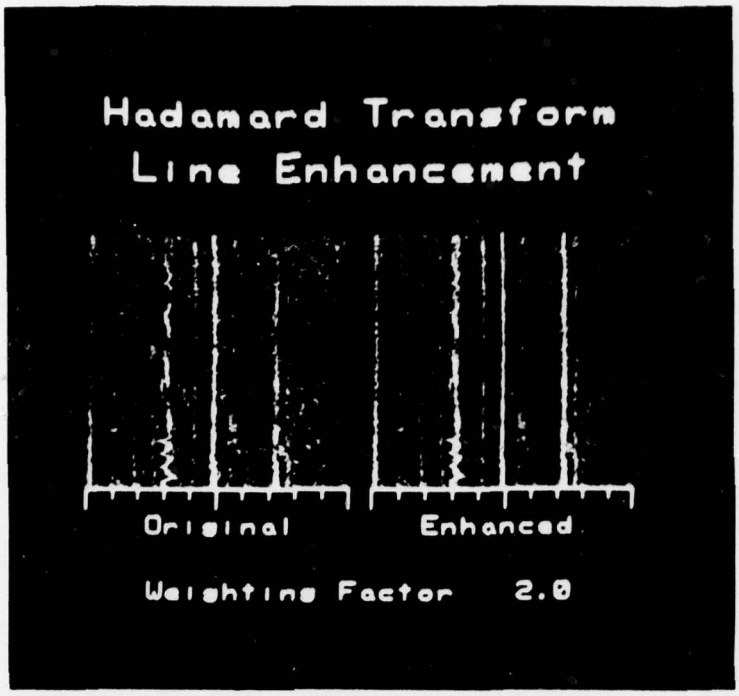

A.
2.0 WEIGHTING FACTOR

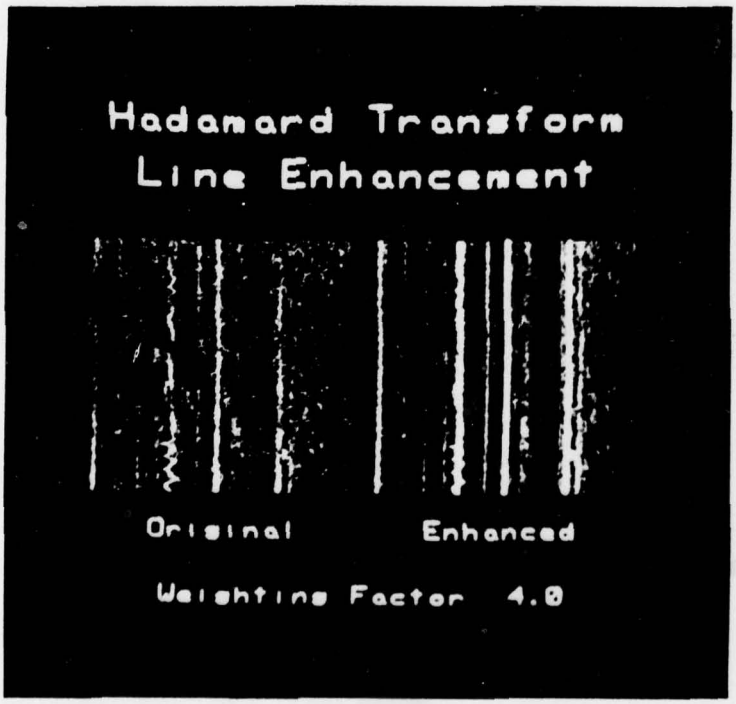

B.
4.0 WEIGHTING FACTOR

Figure 4-2. Comparisons between the source image and Hadamard transform enhanced image reconstructions showing the effects of different weighting factors.

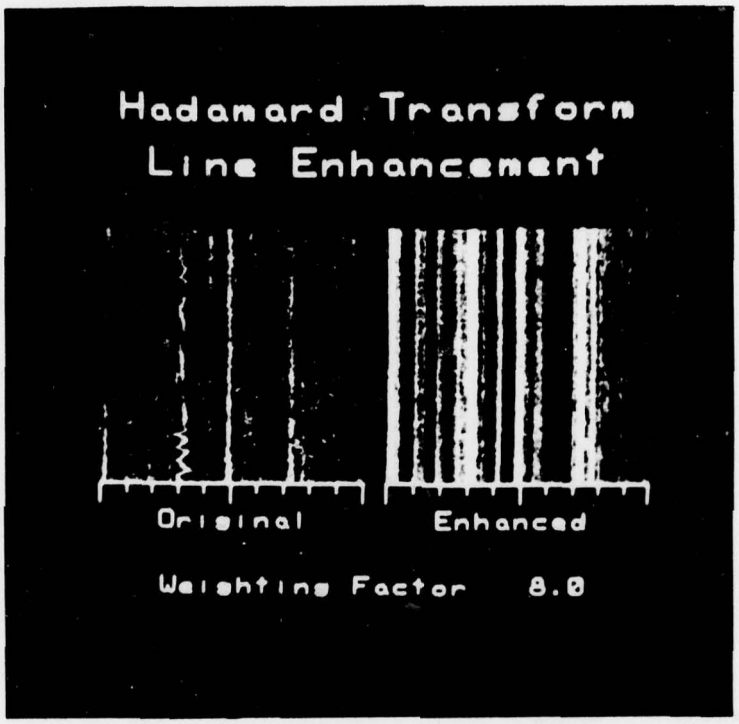

C.
8.0 WEIGHTING FACTOR

Figure 4-2. (Continued)

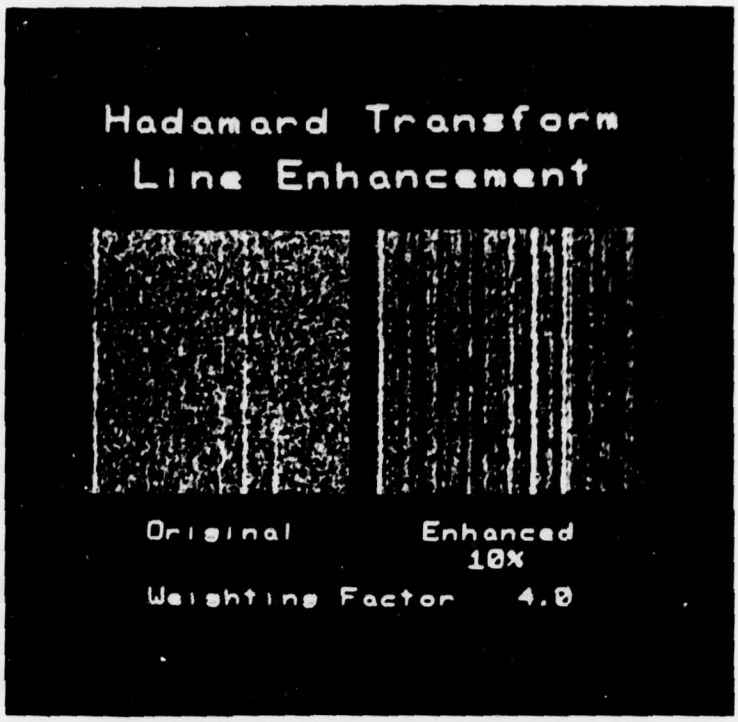

A.
10% OF COEFFICIENTS

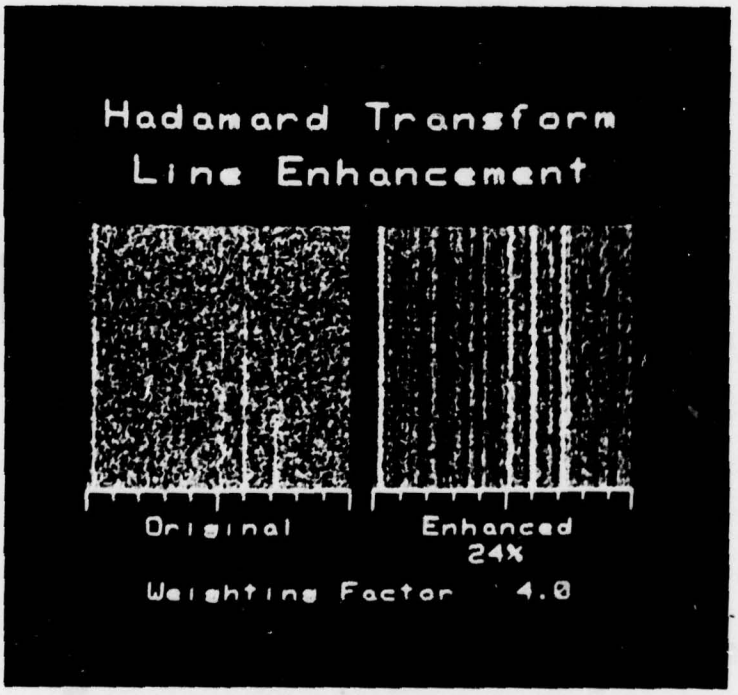

B.
24% OF COEFFICIENTS

Figure 4-3. Comparisons between the source image and Hadamard transform enhanced image reconstructions with the scaling factor applied to different percentages of the d.c. vertical basis function coefficients.

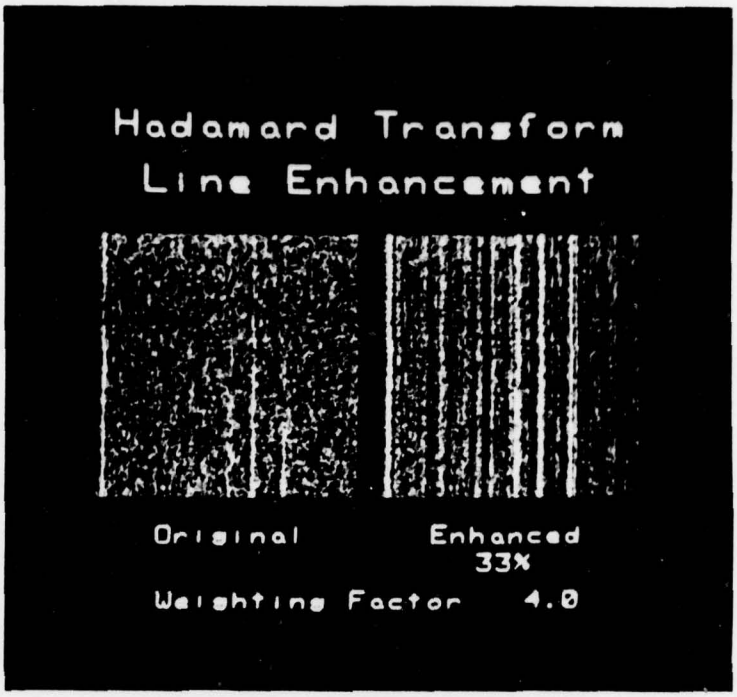

A.
33% OF COEFFICIENTS

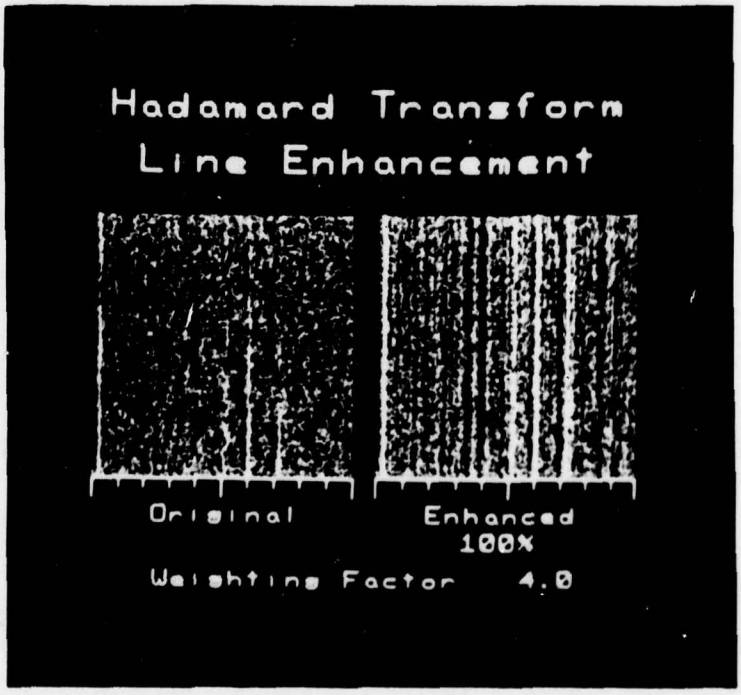

B.
100% OF COEFFICIENTS

Figure 4-3. (Continued)

The third evaluation consists of comparisons between the set of noise-degraded representations of the source image and the image reconstructions with line enhancement. In the first series of comparisons, each noise-degraded source image is compared with the corresponding enhanced image reconstruction using all d.c. vertical coefficients at the same SNR level. These comparisons are illustrated in Figures 4-4a through d.

In each case considered, a significant increase in the detectability of vertical line structures was observed in the enhanced image reconstruction. An example of particular interest is Figure 4-4d, where the lines are no longer detectable in the source image. However, even at this low SNR level, the enhanced image reconstruction indicates the presence of the major source image line structures.

The line enhancement examples presented in Figures 4-2 and 4-4 used all of the d.c. vertical basis function coefficients. As such, the Hadamard transform, results presented could have also been obtained by using the image domain line enhancement procedures given in Appendix D.

Although the above evaluations are subjective in nature and must be considered as preliminary, they do indicate a strong potential for increasing the detectability of vertical line structures in spectral time history images by means of image processing techniques.

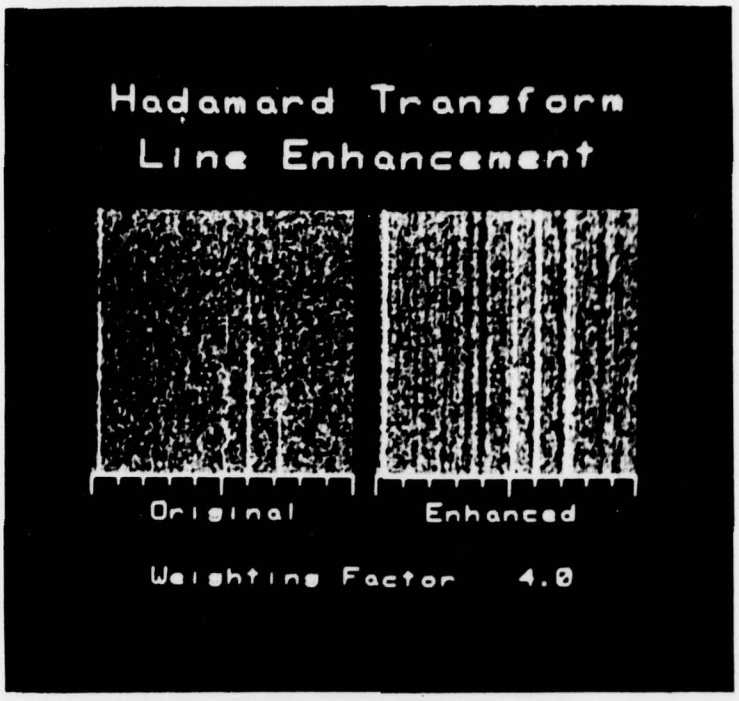

A.

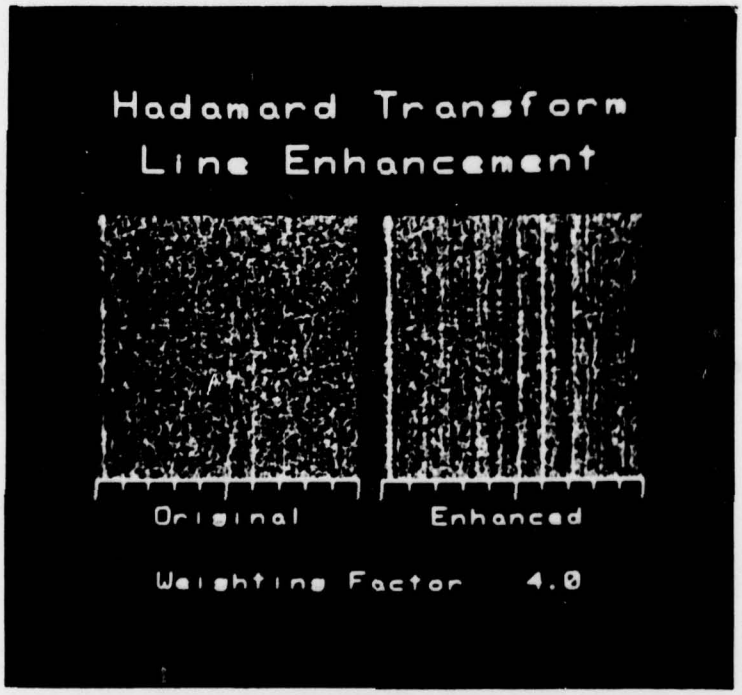

B.

Figure 4-4. Comparisons at the same SNR levels between noise-degraded source versions of the source image and Hadamard transform enhanced image reconstructions. Significant enhancement of vertical lines can be seen for each comparison.

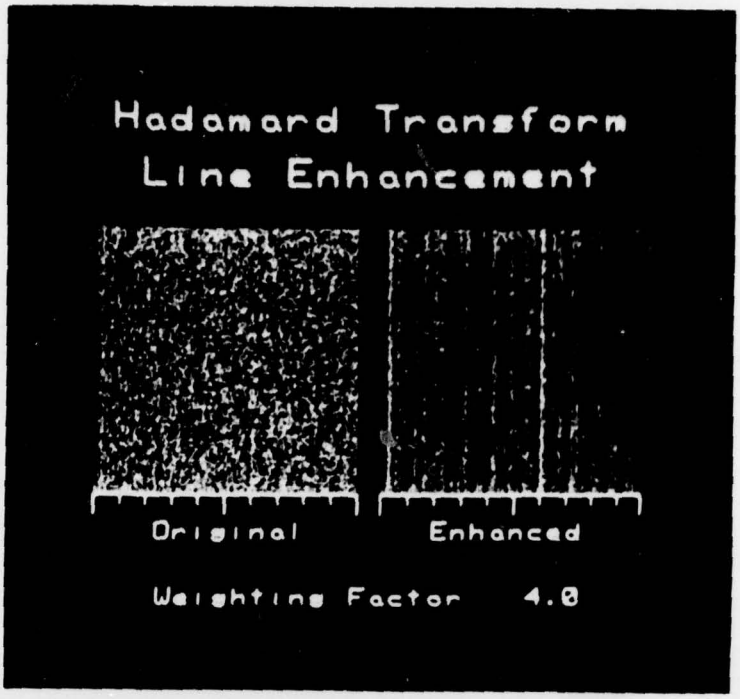

C.

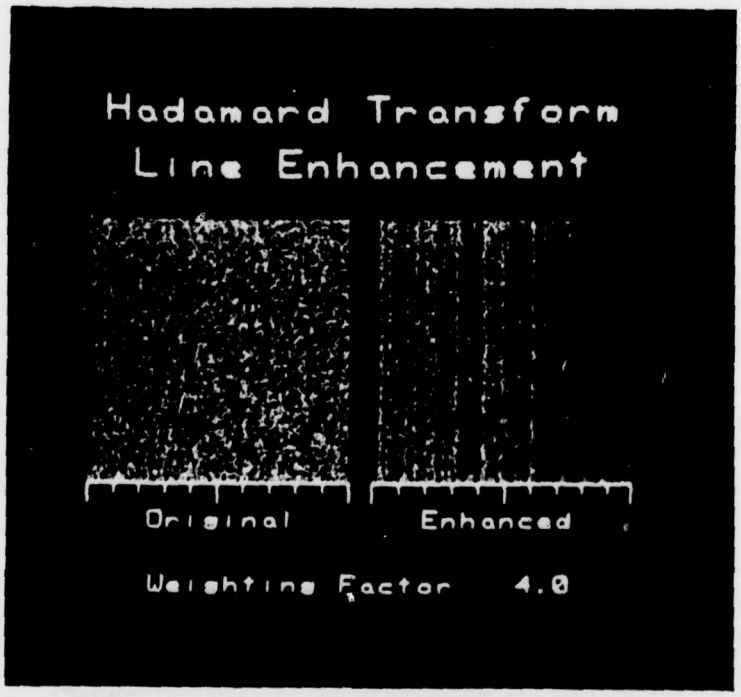

D.

Figure 4-4. (Continued)

SECTION 5 – CONCLUSIONS

The intent of this program effort has been to demonstrate the application of two-dimensional transform processing techniques to acoustic signal space imagery. It has been shown that transform processing gives the acoustic image analyst an extremely versatile and powerful set of investigative tools. The continued development and refinement of this class of processing techniques for acoustic signal space images is highly recommended.

Specific conclusions resulting from this effort include the following:

- The basis functions of the Fourier and Hadamard transforms are well suited to transform domain analysis of acoustic signal space imagery.
- Extension of one-dimensional time series filtering concepts to two-dimensional spatial frequency filtering is an effective technique for analysis of acoustic signal space imagery.
- The concept of transform domain pattern modification is a powerful technique for selective enhancement or suppression of spatial features within an acoustic signal space image.
- The techniques of transform domain analysis are well suited to a highly interactive approach for performing acoustic signal space image analysis operations.
- Hadamard transform domain line enhancement can produce significant gains in the detectability of vertical line structures in spectral time history images.
- Under specified circumstances, Hadamard transform domain and image domain techniques for vertical line enhancement are mathematically equivalent.

APPENDIX A – DISPLAY AND IMAGE PROCESSING FACILITY

BACKGROUND

The NOSC Display and Image Processing Laboratory shown in Figure A-1 is a user-oriented research facility for the analysis and display of digital and video imagery. Laboratory facilities are used in a variety of applications requiring display of natural and computer-processed images and real-time video. Displays of computer-processed imagery include various format options for time sequence presentations of surveillance sonar data, situation displays for system performance prediction, and deformation modeling of sonar transducers. Natural image displays include digitized multi-spectral satellite imagery, encoded aerial reconnaissance sequences, and X-ray fluoroscopy. In addition, laboratory resources include a three-dimensional real-time color video system. This system has been used with a NOSC unmanned submersible work vehicle to evaluate three-dimensional video in an operational undersea environment. Other Laboratory activities include research programs on two-dimensional processing techniques for digital image analysis and enhancement and computer-generated stereoscopic imagery.

DISPLAY HARDWARE

Display devices in the Display and Image Processing Laboratory include:

- COMTAL 8300 Digital Image Display
- Digital-to-Video Image Conversion System
- ADVENT 1000A Videobeam *projection* system
- VARIAN STATOS V electrostatic printer/plotter
- MAGNAVOX color television camera (2 units)
- HONEYWELL stereoscopic viewers (3 units)
- SONY 2850 editing video tape recorder
- SONY color monitors (2 units)
- TEXTRONIX 4014 graphics display terminal
- NIKON and POLAROID cameras
- GAMMA SCIENTIFIC spectro-radiometric instrumentation

The principal Laboratory display device is the COMTAL 8300 Digital Image Display system. This system provides the user with the capability to display and interactively manipulate high-resolution color images. Pertinent features of the COMTAL system include:

- 512 X 512 picture element (pixel) resolution with a 1:1 aspect ratio
- Selectable data display modes, including gray scale, pseudocolor, and true color
- Three independent images stored at one time
- Eight bits of intensity coding stored for each pixel (six bits displayed)
- Graphics overlay for superimposing outlines, grids, or alphanumerics on display images
- Trackball positioning of a target pointer using a trackball input control device

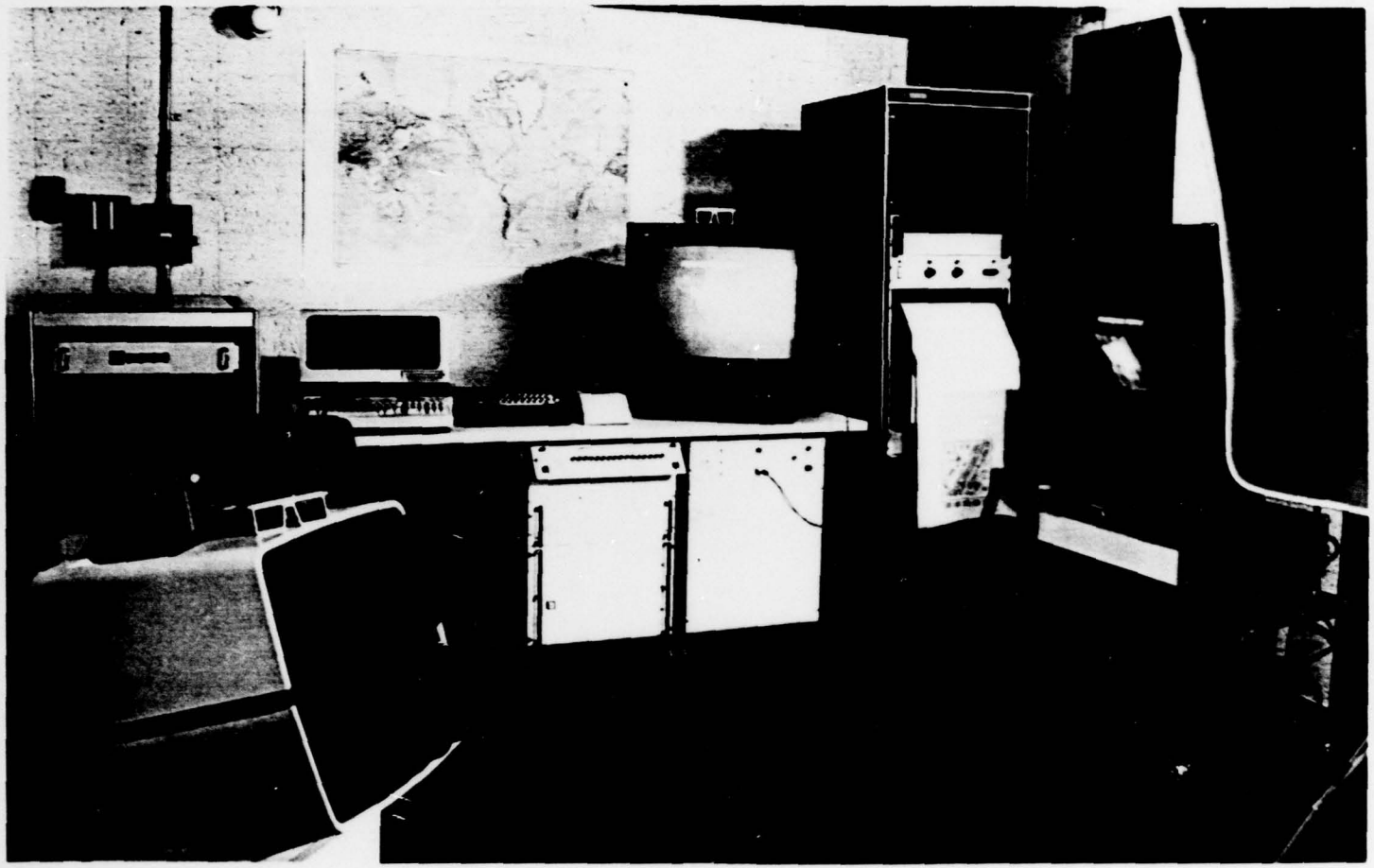

Figure A-1. Display and Image Processing Facility.

In conjunction with the COMTAL system, a digital-to-video image conversion system has been developed for producing NTSC compatible color video tape cassettes of images displayed on the COMTAL. This system is called the Computer-Generator Video Tape system (CVT). Tapes produced on the CVT system can be played on any standard video playback/monitor unit. With this system, results of current COMTAL display simulations or experiments can be made available for immediate presentations outside of the laboratory.

DISPLAY AND IMAGE PROCESSING SOFTWARE

Extensive user-oriented software has been developed in support of Display and Image Processing Laboratory activities. An operating system supported by a library of FORTRAN callable user routines has been written for the COMTAL 8300 system. Using this system, highly interactive operations involving data retrieval and editing, alphanumeric and graphic overlay generation, trackball target control, and image manipulation using function memory modification can be performed on demand terminals located in the Laboratory area. In addition, many user application routines exist, including algorithms for transform and spatial domain image processing, continuous surface graphics, automatic scoring and analysis of experiments, and image formatting for computer-processed and natural images, stereoscopic imagery and high-refresh-rate loading of image sequences.

In the area of image processing, applications software has been developed to perform one- and two-dimensional discrete Fourier, cosine, slant and Hadamard unitary transforms. Much of this software is designed for interactive operator specification of transform domain filtering operations using two-dimensional low-pass, high-pass, band-reject and band-pass filters. Frequency domain filtering can be used for image noise removal and feature enhancement such as improving edge or contour definition. A similar set of algorithms has also been implemented for processing in the original image domain. These methods include techniques for image domain spatial noise removal, edge detection, and contrast enhancement.

User software also exists for the auxiliary STATOS V electrostatic printer/plotter and for the TEXTRONIX 4014 graphics terminal. The UNIVAC 1108 host computer operated in batch or time share modes from Laboratory demand terminals. The 1108 computer facility offers bulk data storage (disc, drum, 7- and 9-track tape), a high-level operating system (EXEC-8), a selection of standard compilers, including an extended version of FORTRAN 4 (RFOR), and complete mathematical and plotter user libraries (e.g., IMSL, DISSPLA).

APPENDIX B: MATHEMATICAL FORMULATIONS FOR TWO-DIMENSIONAL TRANSFORMS

GENERAL FORMS

The general forms for the two-dimensional forward and inverse transformations of an image array are given in Equations (B-1) and (B-2). The two-dimensional transform of an N X N image array its itself an N X N array of transform domain coefficients. The forward two-dimensional transform operation is

$$F(u,v) = \sum_{x=1}^{N} \sum_{y=1}^{N} f(x,y)\, a(x,y,u,v) \tag{B-1}$$

where a(x,y,u,v) is the forward transform kernel and x,y and u,v are, respectively, image domain and transform domain coordinates. The inverse transform is given by

$$f(x,y) = \sum_{u=1}^{N} \sum_{v=1}^{N} F(u,v)\, a^{-1}(x,y,u,v) \tag{B-2}$$

where $a^{-1}(x,y,u,v)$ is the inverse transform kernel.

The transform kernel a(x,y,u,v) is called separable if it can be expressed in the form

$$a(x,y,u,v) = a_x(x,u)\, a_y(y,v) \tag{B-3}$$

Computationally, transform kernel separability means that a two-dimensional transform of an image can be performed by first applying a one-dimensional transform along the rows of f(x,y)

$$F(u,y) = \sum_{x=1}^{N} f(x,y)\, a_x(x,u) \tag{B-4}$$

followed by another one-dimensional transform along the columns of F(u,y) which yields F(u,v), i.e.,

$$F(u,v) = \sum_{y=1}^{N} F(u,y)\, a_y(y,v) \tag{B-5}$$

Thus, transformations of two-dimensional image arrays reduce to the application of sequential one-dimensional transform algorithms along the rows and columns of the image array.

FOURIER TRANSFORMS

The two main classes of unitary transformations which have been applied to acoustic source images are the Fourier and Hadamard transforms. For the Fourier transform, the general forms for the forward and inverse transforms become

$$\mathcal{F}(u,v) = \frac{1}{N^2} \sum_{x=1}^{N} \sum_{y=1}^{N} f(x,y) \exp\left[\frac{-2\pi i}{N}(ux + vy)\right] \tag{B-6}$$

and

$$f(x,y) = \sum_{u=1}^{N} \sum_{v=1}^{N} \mathcal{F}(u,v) \exp\left[\frac{2\pi i}{N}(ux + vy)\right] \tag{B-7}$$

The two-dimensional discrete Fourier transform can be computed using sequential one-dimensional transform algorithms since its transform kernel is separable and symmetric, i.e.,

$$\exp\left[\frac{2\pi i}{N}(ux + vy)\right] = \exp\left[\frac{2\pi i}{N} ux\right] \exp\left[\frac{2\pi i}{N} vy\right] \tag{B-8}$$

Unitary transformations result in the projection of an imput image into a new orthogonal vector space. In the case of the discrete Fourier transform, the vector space basis functions are complex exponentials.

HADAMARD TRANSFORMS

For the discrete Hadamard transform with basis functions ordered according to increasing sequency, the forward transform assumes the form

$$\mathcal{H}(u,v) = \frac{1}{N^2} \sum_{x=1}^{N} \sum_{y=1}^{N} f(x,y) (-1)^{\sum_{i=0}^{n-1} [g_i(u)x_i + g_i(v)y_i]} \tag{B-9}$$

where

$$n = \log_2 N$$

$$g_0(u) = u_{n-1} \qquad g_0(v) = v_{n-1}$$

$$g_1(u) = u_{n-1} + u_{n-2} \qquad g_1(v) = v_{n-1} + v_{n-2}$$

$$g_2(u) = u_{n-2} + u_{n-3} \qquad g_2(v) = v_{n-2} + v_{n-3}$$

$$\vdots \qquad\qquad \vdots$$

$$g_{n-1}(u) = u_1 + u_0 \qquad g_{n-1}(v) = v_1 + v_0$$

and x_i, y_i, u_i, v_i are the coefficients of the binary expansions of the variables x,y,u,v, respectively.

The two-dimensional Hadamard transform also has the property of row and column separability. Thus, two-dimensional Hadamard image transformations can also be computed using sequential one-dimensional transform algorithms.

APPENDIX C – SPATIAL FREQUENCY FILTERING

GENERAL FORM

The general form for the reconstruction of an image after transform domain filtering is

$$\hat{f}(x,y) = \sum_{u=1}^{N} \sum_{v=1}^{N} F(u,v)\, a^{-1}(x,y,u,v)\, \beta(u,v) \tag{C-1}$$

where $\hat{f}(x,y)$ is the filtered image reconstruction and $\beta(u,v)$ is a two-dimensional set of filter weights. The values assumed by the filter weights determine the spatial features that are eliminated, enhanced, or in some way modified in the reconstructed version of the image.

LOW-PASS FILTER

For the simple case of two-dimensional low-pass spatial frequency filtering, $\beta(u,v)$ has the form

$$\beta_{LP}(u,v) = \begin{cases} 1 & \begin{matrix} u \leq U_{Low} \\ v \leq V_{Low} \end{matrix} \\ 0 & \text{otherwise} \end{cases} \tag{C-2}$$

where U_{Low} and V_{Low} define the bounds for the spatial frequency components used in the image reconstruction. In low-pass filtering, the image reconstruction no longer contains horizontal and vertical spatial frequency components exceeding U_{Low} and V_{Low}. The resulting visual effect of low-pass spatial frequency filtering is a general smoothing of the reconstructed image since the higher spatial frequency components have been removed.

HIGH-PASS FILTER

In a similar fashion, high-pass spatial frequency filtering can be obtained with weights of the form

$$\beta_{HP}(u,v) = \begin{cases} 1 & \begin{matrix} U_{High} \leq u \\ V_{High} \leq v \end{matrix} \\ 0 & \text{otherwise} \end{cases} \tag{C-3}$$

Visually, the result of high-pass spatial frequency filtering is that the bias and low-frequency components less than U_{High} and V_{High} have been removed, leaving just the outlines of image intensity transitions. In the context of the analysis and enhancement of natural images, high-pass filtering is commonly used for edge detection and line enhancement purposes.

BAND-PASS FILTER

The properties of low-pass and high-pass filters can be combined to form two-dimensional band-pass spatial frequency filters. The band-pass filter weights are

$$\beta_{BP}(u,v) = \begin{cases} 1 & \begin{array}{l} U_{Low} \leq u \leq U_{High} \\ V_{Low} \leq v \leq V_{High} \end{array} \\ 0 & \text{otherwise} \end{cases} \tag{C-4}$$

Band-pass filtering is a powerful processing tool because it permits individual image features to be isolated from the remainder of the image. The isolated features of the image can then be analyzed and measured to determine their respective contributions to the original image. Simultaneous implementation of multiple band-pass filters can be used to analyze interactions between combinations of specific spatial features within the image.

BAND-REJECT FILTER

The complement of band-pass filtering is band-reject filtering. The expression for two-dimensional band-reject filter weights is

$$\beta_{BR}(u,v) = \begin{cases} 0 & \begin{array}{l} U_{Low} \leq u \leq U_{High} \\ V_{Low} \leq v \leq V_{High} \end{array} \\ 1 & \text{otherwise} \end{cases} \tag{C-5}$$

This form of spatial frequency filtering allows selective removal of image features while preserving the basic structure of the residual image. By means of this technique, image features attributable to known phenomena can be effectively eliminated to permit an unobscured view of the signal structures of primary interest.

PATTERN MODIFICATION

A special case of spatial frequency filtering are those filters that permit relative adjustments to be made in individual patterns or spatial features of the image. These filters permit variable enhancement or suppression of specific image features by the use of weights of the form

$$\beta_{PM}(u,v) = \begin{cases} \psi & \begin{matrix} U_{Low} \leq u \leq U_{High} \\ V_{Low} \leq v \leq V_{High} \end{matrix} \\ 1 & \text{otherwise} \end{cases} \qquad \text{(C-6)}$$

where $\psi > 1$ results in increased values for the selected components in the transform domain energy distribution and $\psi > 1$ causes a corresponding component value decrease. Such distortions of the transform domain energy distribution produces, respectively, increases or decreases in the perceived strength of the affected features in the image reconstruction. Pattern modification is a potentially powerful image processing tool which can be used to enhance weak features or suppress undesirable ones for subsequent image feature analysis and measurement.

ENERGY RATIO MEASUREMENT

The techniques of spatial frequency filter provide a direct method for evaluating the relative strength of individual spatial features within the source image. The energy ratio measurement has the form

$$\text{Energy Ratio} = \frac{\sum_{u=o}^{N} \sum_{v=0}^{N} |F(u,v)| \beta(u,v)}{\sum_{u=0}^{N} \sum_{v=0}^{N} |F(u,v)|} \qquad \text{(C-7)}$$

where $\beta(u,v)$ is the set of filter weights discussed previously. The numerator of Equation (C-7) represents the energy of a particular feature after filtering, while the denominator is the total energy of the source image. This fractional energy ratio is one of the feature parameters displayed in the lower left quadrant of the spatial frequency filtering display format.

APPENDIX D – IMAGE DOMAIN LINE ENHANCEMENT

In the special case of Hadamard transform attribute modification in which the values of all of d.c. vertical basis function terms are simultaneously adjusted, the equivalent result can be achieved in a computationally simpler manner using image domain processing.

The relationship between the Hadamard transform and image domain vertical line enhancement is developed as follows. From the general form for the forward two-dimensional transform given in Appendix B,

$$F(u,v) = \sum_{x=1}^{N} \sum_{y=1}^{N} f(x,y)\, a(x,y,u,v) \tag{D-1}$$

and, assuming separability of the transform kernel,

$$F(u,v) = \sum_{x=1}^{N} \sum_{y=1}^{N} f(x,y)\, a_x(x,u)\, a_y(y,v) \tag{D-2}$$

where F(u,v) is the transform domain representation of the source image, f(x,y).

The vertical Hadamard transform d.c. values, F(u,0) are given by

$$F(u,0) = \sum_{x=1}^{N} \sum_{y=1}^{N} f(x,y)\, a_x(x,u)\, a_y(y,0) \tag{D-3}$$

where $a_y(y,0) = 1$. Thus, F(u,0) becomes

$$F(u,0) = \sum_{x=1}^{N} \sum_{y=1}^{N} f(x,y)\, a_x(x,u) \tag{D-4a}$$

$$= \sum_{x=1}^{N} a_x(x,u) \sum_{y=1}^{N} F(x,y) \tag{D-4b}$$

or, for notational convenience,

$$= \sum_{x=1}^{N} a_x(x,u)\, f_I(x) \tag{D-4c}$$

The interpretation of Equation (D-4) is that F(u,0) is the column-wise integration over y followed by the transform over x. The inverse transform of F(u,0) is then

$$F^{-1}(u,0) = \sum_{u=1}^{N} \sum_{v=1}^{N} F(u,0)\, a^{-1}(x,y,u,v) \tag{D-5a}$$

$$= \sum_{u=1}^{N} F(u,0)\, a_u^{-1}(x,u) \sum_{v=1}^{N} a_v^{-1}(y,v) \qquad \text{(D-5b)}$$

$$= f_I(x) \cdot \text{unit}(y) \qquad \text{(D-5c)}$$

The reconstruction of the entire image $f_R(x,y)$ is

$$f_R(x,y) = [\, aF(u,v) + bF(u,0) \,]^{-1} \qquad \text{(D-6a)}$$

$$= af(x,y) + bf_I(x) \cdot \text{unit}(y) \qquad \text{(D-6b)}$$

where the constants and and b define the relative weights assigned to the entire image (normally a = 1) and to the inverse of the vertical transform domain d.c. values.

However, since $f_I(x)$ is simply the integration over y at each x location, the computation of $f_R(x,y)$ can be performed entirely in the image domain with a significant reduction in computational requirements. Thus, the image domain equivalent of Hadamard transform line attribute modification using all vertical d.c. values is to combine the original spectral time history source image with a weighted computation of $f_I(x) \cdot \text{unit}(y)$.